(NASA-CR-194580) HIGH TEMPERATURE CO-AXIAL WINDING TRANSFORMERS Final Interim Report, May 1992 - Feb. 1993 (Wisconsin Univ.) 57 p

N94-19643

NASA-CR-194580

Unclas

G3/33 0190552

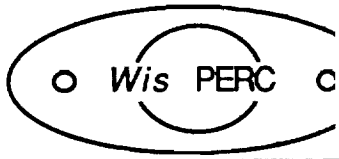

Wisconsin Power Electronics Research Center

NASA Grant Report

HIGH TEMPERATURE CO-AXIAL WINDING TRANSFORMERS

Cooperative Agreement No. NCC3-261
Final Report

University of Wisconsin - Madison
Department of Electrical and Computer Engineering
Madison , WI 53706

Deepakraj M. Divan
Donald W. Novotny
Principal Investigators

Nasser H. Kutkut
Project Engineer

prepared for

NASA LEWIS RESEARCH CENTER
Cleveland, OHIO 44135

Eric Baumann
NASA Grant Manager

For the Period
May 1992 to February 1993

TABLE OF CONTENTS

Chapter 1

CO-AXIAL WINDING TRANSFORMERS FUNDAMENTALS

1.1 Introduction

An important concern in high frequency electronic power conversion is the question of magnetic component design, particularly at higher power levels. The question of how to realize high-power high-frequency transformers has been particularly daunting. In order to achieve reasonable performance, it is necessary to obtain very low leakage inductances, while simultaneously ensuring that the leakage flux is not concentrated in a small section of the core. Further, transformer designs which feature easily predictable leakage inductances are appealing for use in soft switching circuits in which the leakage inductance is a useful circuit component.

Co-axial winding transformers (CWT) have been used for many years in microwave applications because of their extremely low leakage inductances. The use of co-axial winding transformers for high-frequency, high-power converters was proposed in reference [1]. The co-axial transformer concept has been used with considerable success in various converters including a 50 kHz, 50 kW dual active bridge dc/dc converter and a 600 watt, 1 MHz dual resonant dc/dc converter [2,3]. The design of such co-axial transformers is considerably different from that of conventional transformer structures.

The basic co-axial transformer arrangement is shown in Fig. 1.1. The outer conducting tube forms one of the windings. The inner winding is wound completely inside the outer conductor. Integral turns ratios are possible by using multiple turns on the inner winding. The magnetic core is completely outside of the outer conductor. Variations of the basic arrangement in Fig. 1.1 are possible which provide multiple turns on the outer winding.

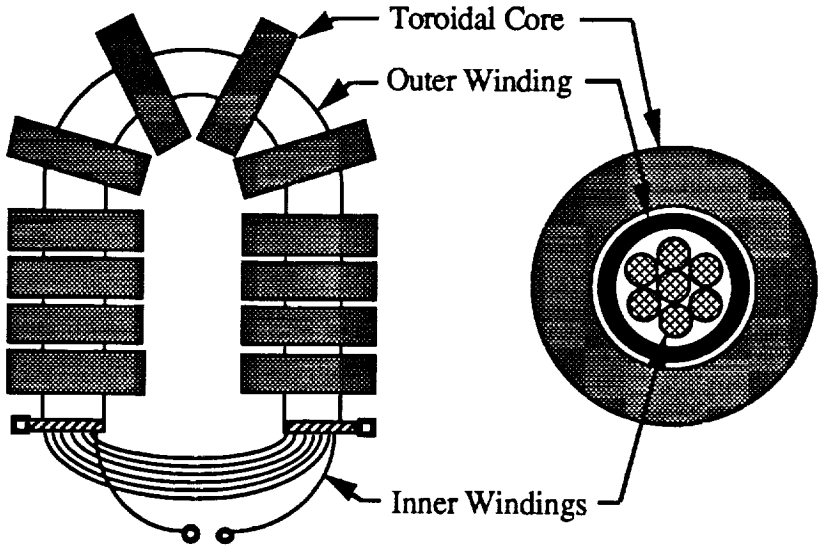

Fig. 1.1 Co-axial transformer arrangement.

Qualitatively, the transformer works as follows: Assume that a voltage is applied at the outer winding of Figure 1.1. (For illustrative purposes the outer winding is considered the primary. However, either winding can be used as the primary). This will produce a magnetizing current, I_m as shown in the cross sectional diagram of Figure 1.2. The resulting flux will be tangential to circular paths outside of the outer winding. All flux produced by the outer winding links the inner winding. The converse is essentially true when the relative permeability of the core is many times the permeability of the space between the inner and outer windings. In either case the majority of flux produced by one winding will link with the other winding and induce a voltage proportional to the applied voltage times the turns ratio of the windings.

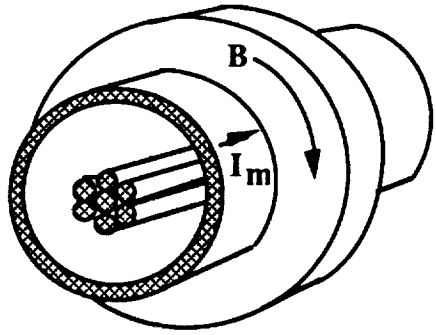

Fig. 1.2 Magnetizing current and mutual flux of the transformer

1.2 Flux Distribution and Core Loss

A common assumption used in transformer design is to assume that the flux density throughout the core is constant because it simplifies design computations related to the magnetizing current and the core loss. However, the actual flux density in any transformer core is never exactly uniform.

For the co-axial transformer, the core flux distribution is well defined and controlled. Essentially none of the leakage flux finds its way into the core. However, the core flux distribution is not uniformly spread across the radius of the core, which indicates that core loss depends on the ratio of the toroidal core inner (r_{ci}) and outer (r_{co}) radii. The approximate flux distribution for the co-axial transformer is shown pictorially in Fig. 1.3. It was shown by Rauls [4] that the core loss calculation which assumes uniform flux density is actually larger than the one which uses the non-uniform flux distribution. Hence, estimates for the core loss with the constant flux density assumption are conservative estimates.

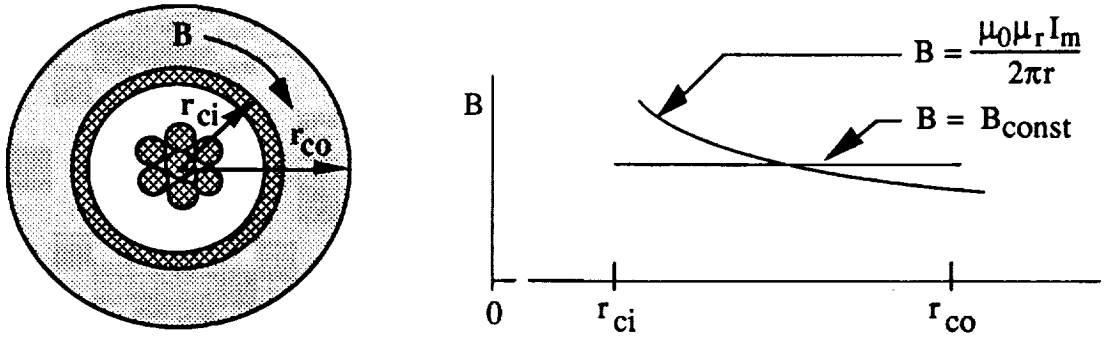

Fig. 1.3 Flux density as function of radius for non-uniform and uniform flux distribution.

1.3 Co-axial Transformer Inductances

One of the main advantages that the co-axial winding transformer has over a conventional transformer design is its very much lower leakage reactance which is also easily calculated and controllable. The fact that it is controllable lends itself to use in soft switching circuits where the transformer leakage inductance is used as the resonant inductor in the

circuit. This sections examines the leakage and magnetizing reactance properties of the co-axial transformer and develops an equivalent circuit model.

1.3.1 Magnetizing Inductance

The magnetizing inductance for the co-axial transformer is calculated by assuming that all mutual flux is contained within the transformer core. To find the magnetizing inductance, a current (I) is assumed in the primary winding which has N_1 turns and the secondary is assumed to be an open circuit. The relevant geometry is shown in Figure 1.4.

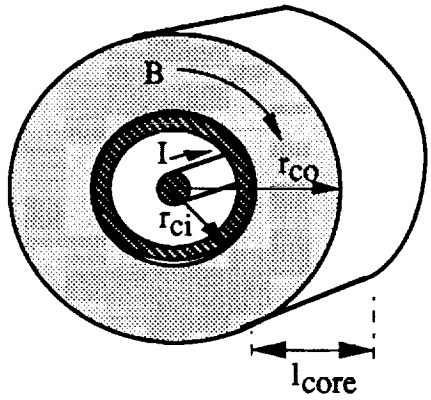

Figure 1.4 Magnetizing current and mutual flux of the transformer.

By using Ampere's law to compute the total flux and the flux linkage, the magnetizing inductance is found to be,

$$L_m = (N_1)^2 \frac{l_{core}\mu_0\mu_r}{2\pi} \ln\left(\frac{r_{co}}{r_{ci}}\right) \approx (N_1)^2 \frac{l_{core}\mu_0\mu_r}{\pi} \frac{r_{co}-r_{ci}}{r_{co}+r_{ci}} \qquad (1.1)$$

Notice here that the above analysis assumes nearly constant permeability in addition to no core saturation. The intent of (1.1) is to give a good estimate of the mutual inductance so that a relative comparison can be made with the leakage inductance of the transformer.

1.3.2 Transformer Leakage Inductance

Leakage inductance is the inductance resulting from flux in one winding which does not mutually link another winding. For co-axial transformers, if co-axial symmetry is

maintained between the windings over the entire length of transformer, the problem of calculating the leakage inductance can be treated as a two dimensional one. For co-axial winding transformers with end turns that do not maintain co-axial symmetry, three dimensional analysis is needed. The leakage reactance per unit length is determined by using the specific permeance concept which is used by Lipo [5].

Figure 1.5 shows a co-axial transformer cross section with seven turns on the inner winding and one turn on the outer winding. The inner winding leakage consists of three components. First, there is a leakage reactance due to the flux within the inner winding space which is the internal self inductance of the inner winding. Second, the space between the inner and outer windings contains inner winding flux which does not link the outer winding. Third, there is a component due to the finite thickness of the outer wall.

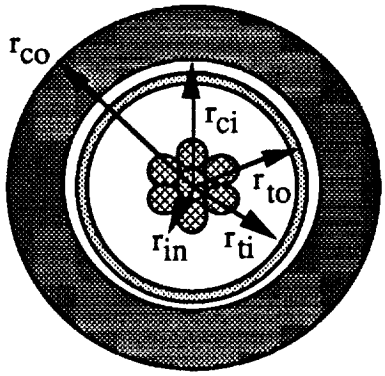

Figure 1.5 Transformer cross section

By applying the permeance analysis concept, the co-axial transformer leakage inductance can be calculated. It was shown by Rauls [4] that if the excitation frequency is sufficiently high so that all of the current is crowded within a thin skin at r_{ti}, or if the actual thickness of the outer winding wall is small relative to r_{ti}, the inner winding leakage inductance is calculated to be,

$$L_{leak\_in} = \frac{N_s^2 \mu_o}{8\pi}\left(1 + 4\ln\left(\frac{r_{ti}}{r_{in}}\right)\right) l_{turn} \qquad (1.2)$$

which is the inductance for a co-axial transmission line when N_S is set to one. In order to minimize the leakage inductance, the space between the inner and outer windings should be

kept small. Also, notice that multiple turns for the inner winding increases the inner winding leakage inductance by the square of the series connected turns.

Note here that the leakage on the inner winding side results from flux produced by the inner winding which does not link the outer winding completely. From the outer winding side all flux produced by the outer winding will link the inner winding because all of the flux is located outside of r_{ti}. Hence, there is no leakage reactance on the outer winding side.

1.4 Equivalent Circuit Models

The equivalent electrical circuit model for a transformer can be derived from the equivalent magnetic circuit model by using the duality principle [6]. The magnetic circuit model for a conventional wound transformer is derived along with the corresponding electrical circuit by Selmon in [6]. The electrical model which relates the transformer inductances is repeated below in Figure 1.6.

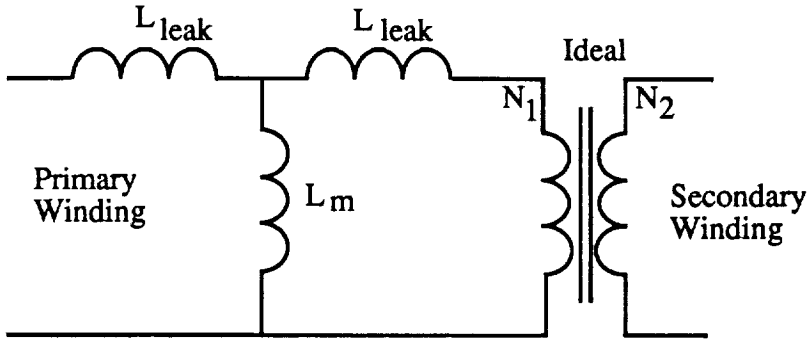

Figure 1.6 Y equivalent circuit model for the conventional wound transformer

This is normally referred to as a Y-equivalent circuit. Notice that the leakage is divided evenly among the winding sides in the Y-equivalent model. Symmetrical division of the leakage in the Y equivalent circuit is typical in conventional transformers .

1.4.1 Two Winding Co-axial Transformer Model

The two winding model for the co-axial transformer can be derived in the same manner as the conventional wound transformer in [6]. The first step is to determine the

magnetic circuit model which is found by examining the mmf and reluctance for each transformer winding. For the outer winding there is only mutual reluctance in the core and a corresponding mmf. For the inner winding there is the mutual core reluctance, the leakage reluctance between the inner and outer winding, and an mmf. The magnetic circuit is shown in Figure 1.7.

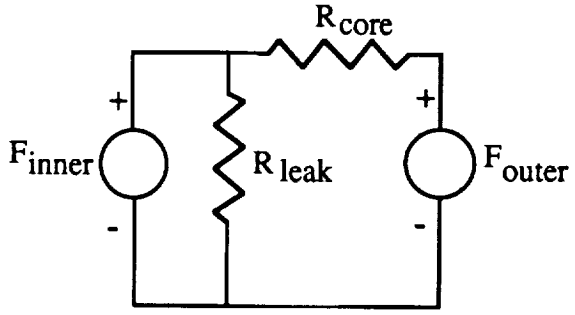

Figure 1.7 Magnetic circuit model for the two turn co-axial winding transformer.

Taking the dual of the circuit in Figure 1.7 and converting it to the electrical equivalent results in the circuit shown in Figure 1.8.

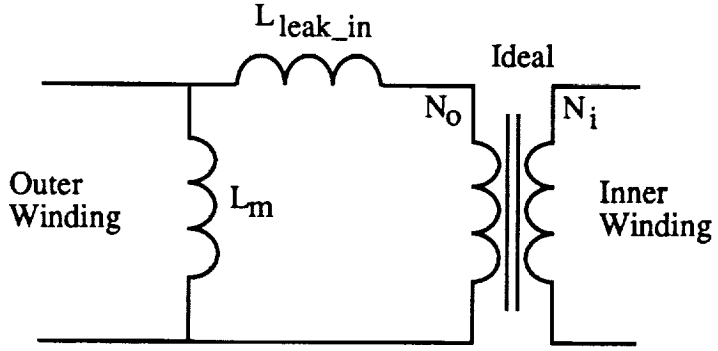

Figure 1.8 Electrical circuit model for the two winding co-axial transformer.

Notice that the circuit model has the leakage inductance distributed differently than the circuit model for the conventional transformer in Figure 1.6. Because all of the outer winding flux is contained within the core, the inner winding leakage term is distributed entirely on the inner winding side of the mutual inductance in the equivalent circuit model. The approximate equivalent magnetizing resistance which models the core loss is defined as,

$$R_m = \frac{V_{rms}^2}{P_{loss\_core}} \tag{1.3}$$

but is only partially correct because at rated voltage there is I^2R loss in the primary which reduces the voltage across R_m to something below the input at the transformer terminals. The equivalent circuit model is shown in Figure 1.9.

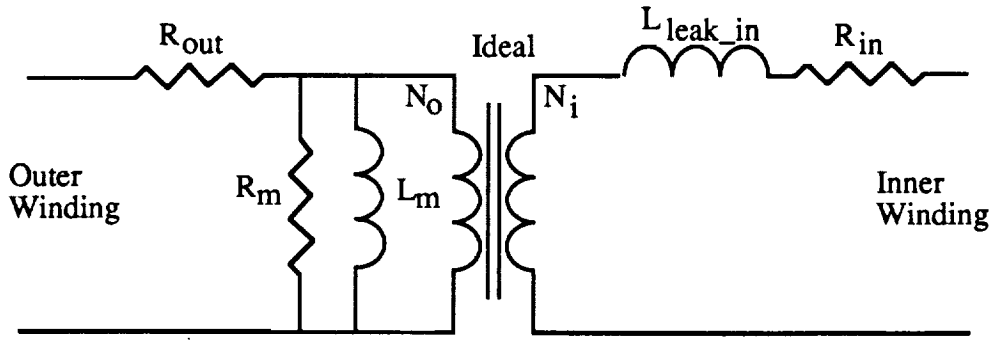

Figure. 1.9 Equivalent circuit model for the two winding co-axial transformer.

1.5 Co-axial Transformer Design

Transformer design can be a challenging task because of the many degrees of freedom which need to be considered simultaneously in a design procedure. Further, the design involves constraints which typically include efficiency, power density, temperature rise and physical dimensions. Most of the design concepts which have been developed for conventional transformers can be applied to the design of a co-axial transformer. However, there are some unique design issues which relate specifically to the co-axial design.

1.5.1 Relation Between The Core Flux And The Voltage

The relation between the primary voltage and the core flux is derived from Faraday's law as,

$$V_{rms} = 4\, K_w N f B_m A_c \qquad (1.4)$$

where A_c is the flux cross sectional area of the core, B_m is the peak flux density, f is the excitation frequency, N is the number of series connected turns in the primary winding, K_w is the wave form shape factor which is 1.11 for sinusoidal excitation or 1.0 for square wave excitation, and V_{rms} is the primary rms voltage. The flux cross sectional area is related to

the toroidal core geometry in a co-axial transformer (by referring to Fig. 10) as,

$$A_c = (r_{co} - r_{ci})l_{core} \tag{1.5}$$

The volume of the core (V_c) is,

$$V_c = \pi(r_{co}^2 - r_{ci}^2)l_{core} \tag{1.6}$$

Note here that equation (1.4) assumes that the flux density is uniform in the core when in fact it is inversely proportional to r. However, it was discussed earlier that a good and conservative estimate of the core loss can be obtained by using a uniform flux density.

Mean length for each turn is approximately $(l_{core} + 2\pi r_{co})$
Transformer length is defined as $\frac{l_{core}}{2}$
Transformer width is defined as $4r_{co}$

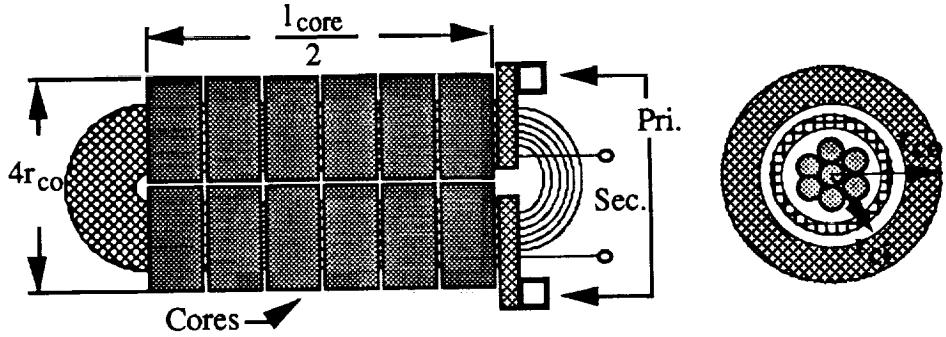

Figure 1.10 Geometry definitions and dimensions for the co-axial transformer.

1.5.2 Core Loss Dependency On Frequency And Flux Density

A general expression for the core loss per unit volume as a function of frequency and flux density is given by,

$$C_{l\_v} = K_c(B_m)^n(f)^m \qquad \text{[W/unit volume]} \tag{1.7}$$

where K_c is the units/scaling constant, n is the flux density exponent near 2.5 for ferrite and 1.9 for metals, m is the frequency exponent which is typically in the range of ($1.0 \leq m \leq 1.6$). The exponents m and n are very material dependent. The total core loss can be found by multiplying (1.6) by (1.7),

$$C_l = \pi(r_{co}^2 - r_{ci}^2)l_{core}K_c(B_m)^n(f)^m \qquad \text{[W]} \tag{1.8}$$

Equation (1.9) is intended only as a tool to help evaluate the transformer design in an iterative optimization process. Once a near optimum design is found, a more accurate reading of the core loss per unit volume is obtained by reading it directly from the core loss plots in the manufacturer's catalog at the particular flux density and frequency of interest. The result is then multiplied by the core volume to determine a more accurate value of the total core loss.

1.5.3 Winding Losses

When litz wire is used in a winding the per unit length ac resistance is determined by direct application of the resistance formulas provided in the manufacturer's catalog. The determination of the ac resistance of tubular windings has been done by Rauls in [4], where expressions for the per unit length ac resistance were presented. Once the per unit length ac resistances are known, the winding losses for the primary (P_{wind_pri}) and secondary (P_{wind_sec}) are determined by straightforward application of Ohm's law,

$$P_{wind\_pri} = I_{pri}^2 R_{ac\_pri} N_1 (l_{core} + 2\pi r_{co}) \qquad (1.9)$$

$$P_{wind\_sec} = I_{sec}^2 R_{ac\_sec} N_2 (l_{core} + 2\pi r_{co}) \qquad (1.10)$$

where the mean winding length per turn has been defined in Figure 1.10, and N_1 and N_2 are the primary and secondary number of turns, respectively.

1.5.4 Trade Offs Between The Different Degrees Of Freedom

This section discusses how the various degrees of freedom affect the co-axial transformer size and performance. It is assumed here that the type of core material remains constant.

The different trade offs can be summarized as follows:

1) Adjusting The Frequency:

By referring to (1.4), it is clear that as f goes up A_C goes down by the same factor if

everything else is fixed. However, the winding losses will go up with frequency for a fixed number of turns and winding window area. It is not clear whether core losses will go up or down and a calculation is needed to see the net result.

2) Adjusting The Length To Width Ratio:

For a fixed number of turns and winding window area, the winding losses will decrease by reducing the winding length which favors a transformer length to width ratio near one. The core loss is minimized by making the length to width ratio as high as possible since for a fixed A_c the volume is minimized as the length tends towards infinity.

3) Adjusting The Number Of Turns:

An increase in the number of turns results in a decrease in A_c if everything else is fixed. Note that both the primary and secondary number of turns must be increased by the same factor if the turns ratio is to remain unchanged. For a constant winding window the total core loss will come down because the core volume is decreased. The winding losses will increase for an increase in the number of turns because the cross sectional area per turn will decrease.

4) Adjusting The Flux Density:

By referring to (1.4), it is clear that as B_m goes up Ac goes down by the same factor if everything else is fixed. Hence, the core volume will go down which reduces the core size, but the core loss per unit volume goes up in (1.8) with flux density. It is not obvious whether the total loss goes up or down and a calculation is needed for that.

5) Adjusting The Winding Window Area:

The winding losses will increase and the core losses will decrease if the winding window area is made smaller while the core length is kept fixed. Since the winding window area is proportional to the square of the winding radii, the per unit length

resistance will increase as the square of the change in the winding radii. The net result is an increase for the winding losses. The total core loss will decrease because the core volume decreases while the core loss per unit volume remains the same.

1.5.5 First Pass Design Procedure

In order to do a first pass design, the transformer kVA, voltages, frequency, and wave form shape must be defined. By considering the performance constraints a choice of core material and flux density can be made. From these initial parameter choices, it is determined if a design is feasible. If the initial design is far away from the target performance, the voltage, frequency, number of turns, and/or core material must be modified to find a better combination of parameters. Once a workable design has been determined, it can be refined by iteration using the remaining degrees of freedom.

The design approaches that can be used in designing transformers are:

1) The Area Product Approach

One method used for initial designs in conventional transformers is to use the so called area product which is defined as,

$$A_c A_w = \frac{2 V_{rms} I_{rms}}{K_w f B_m k_s k_f J_{ave}} \qquad (1.11)$$

where Ac, V_{rms}, I_{rms}, K_w, f, B_m were defined in (1.7), A_w is the winding window, k_s is the core stacking factor, k_f is the winding fill factor, and J_{ave} is the average conductor current density. Core manufacturers often list a parameter in their catalogs called the area product which is proportional to the recommended transformer VA rating which can be handled by the core. This helps the designer select a core size.

2) The Current Density Approach

With some experience the designer can develop an intuition for selecting a current density which is likely to work under the VA and temperature rise constraints. The winding

window is then chosen based on the total current capacity requirements and choice of current density. The outer winding tube size is determined by allowing enough space to fit all of the inner winding turns and any necessary insulation. From equation (1.2), it is clear that the space between the inner and outer winding should be minimized if the inner winding leakage inductance is to be minimized. However, one may want to leave some air space to enhance the cooling capability of the winding.

Figure 1.11 shows the basic procedure used to evaluate a design based on a particular choice of kVA, voltage, frequency, number of turns, and wave form shape. Once the dimensions have been determined the transformer core loss, winding loss, volume, weight, etc. can be determined to see if the transformer meets the requirements of the application.

1) Define kVA, voltages, frequency, number of turns, and wave form shape.
2) Select a core material and flux density appropriate for the application.
3) Determine the inner winding cross section from current rating, current density and # of turns.
4) Select an outer tube size which fits over the inner winding [4].
5) Select an available core geometry which fits over the outer winding.
6) Determine the core area from (1.4)
7) Determine the core length from (1.5)
8) Calculate the losses, volume, weight, etc.
9) If unacceptable, repeat (1-8) after parameters have been modified.

Figure 1.11 Procedure for evaluating the transformer performance.

1.6. Conclusions

In this chapter, the analysis and design of co-axial winding transformers is presented. The design equations were derived and the different design approaches were discussed.

As shown in this chapter, one of the most important features of co-axial winding transformers is the fact that the leakage inductance is well controlled and can be made low. This is not the case in conventional winding transformers. In addition, the power density of co-axial winding transformers is higher than conventional ones. Hence, using co-axial winding transformers in a certain converter topology improves the power density of the converter.

Chapter 2

CO-AXIAL WINDING TRANSFORMER DESIGN

2.1 Introduction

In this chapter, the co-axial winding transformer fundamentals introduced in chapter 1 will be used to design a high temperature co-axial winding transformer for space applications. The specifications for such a transformer will be introduced and the basic design considerations will be discussed. The design algorithm discussed earlier will be employed to iteratively look for an optimal design.

The designed transformer was constructed and tested at room temperature and high temperature environments. Test setups and experimental results will be presented later in this chapter.

2.2 High Temperature Transformer Specifications

The specifications for a proposed 2.5 kVA high temperature transformer are listed in Table 2.1.

Table 2.1 Proposed specifications for a 2.5 kVA high temperature transformer

Base Plate Temperature	200° C
Cooling	Air Cooled / Cold Plate
Frequency	20 kHz, sinusoidal excitation
Voltage Rating	125 V rms input, 125/250 V rms output
Turns Np : Ns	2 : 4 (Split Secondary)
Rating	2.5 kVA
Weight	< 15 lb.

Due to the high ambient temperature in the proposed specifications (200°C), the main design considerations include high Curie temperature magnetic materials (>200°C) in addition to high temperature insulation materials. In the next section, an investigation of some possible magnetic materials will be presented.

2.3 High Curie Temperature Magnetic Materials

In this section, an overview of some possible magnetic materials will be presented. The key issues to consider in selecting a suitable magnetic material for the proposed transformer are:

a) High curie temperature (> 200°C).

b) High flux density levels.

c) Low losses at the specified operating flux and frequency levels.

Although Ferrites have very low losses at high frequencies, they are excluded due to their low curie temperature (< 200°C). By surveying the manufacturer's magnetic materials catalogues, it was found that the tape wound cores are good candidates for such an application. Some of the possible materials investigated that suit this application include: Metglas alloys 2605 SC and 2605 S3A, Square Permalloy 80 and Supermalloy. Typical characteristics of these materials are listed in Table 2.2. The data shown in Table 2.2 was obtained from the MAGNETICS and ARNOLD tape wound core catalogues except for the Metglas 2605 S3A alloy where the data for this alloy was obtained from the ALLIED SIGNAL METGLAS catalogue [7,8,9]. The extensions (MG), (AR) and (AS) will be used to indicate whether the data were obtained from the MAGNETICS, ARNOLD or ALLIED SIGNAL catalogues, respectively. Note also here that the specific core loss data are extrapolated from the specific curve loss curves for 1 mil alloys since no loss curves were provided for 20 kHz operation. The corresponding manufacturer's data are included in appendix A.

By taking a closer look at Table 2.2, it can be seen clearly that even though the Metglas 2605 SC alloy has much higher flux density levels, the corresponding core losses are rather

high. Hence, the material was excluded from further investigation. The rest of the materials listed will be further considered for possible transformer design.

Table 2.2 Typical characteristics for some tape wound materials

Material	Metglas 2605 SC	Metglas 2605 S3A	Square Permalloy	Supermalloy
Catalogue	(MG)	(AS)	(MG)	(MG & AR)
B_saturation (25°C) (Tesla)	1.6	1.4	0.82	0.82 (MG) 0.82 (AR)
Curie Temp. (°C)	370	358	460	460 (MG) 400 (AR)
Density (gm/cm^3)	7.32	7.29	8.71	8.71 (MG) 8.77 (AR)
Relative Permeability	40,000 to 300,000	20,000 to 35,000	10,000 to 100,000	30,000 to 60,000
Core Loss (W/lb.) for 1 mil tape @ 20 kHz, 25°C				
B = 0.4 T	46	14	18	17 (MG)
0.5 T	70	23	25	23 (MG)
0.6 T	90	32	30	33 (MG)
0.7 T	130	41	---	---
0.8T	160	55	---	---
1.0 T	180	91	---	---

2.4 Co-axial Winding Transformer Design

At this stage, and given the specifications proposed earlier, a first pass transformer design can be attempted. The current density design approach discussed earlier in chapter one will be employed. An optimal design can then be obtained by using the iterative algorithm proposed in Fig. 1.11.

In order to obtain a first pass design, the current density for the primary and secondary windings, the flux density level in the core in addition to the primary and secondary turns need

to be specified first. Specifying the current density in such applications should take into consideration the total copper loss generated, the temperature rise in the copper in addition to cooling techniques. However, good experience in designing transformers enables the designer to select a reasonably acceptable current density level for a certain application. Typical current density levels that are used in designing co-axial winding transformers are **400 A/cm^2** for the inner winding wire and **600 A/cm^2** for the outer winding tube. The higher current density for the outer winding stems from the fact that more area is exposed to outer media or cold plate. Hence, these levels will be used to come up with a first pass design.

In specifying the flux density level, it was shown in chapter 1 that increasing the flux density level tends to decrease the required core cross sectional area by the same factor if every thing else is kept constant. On the other hand, the core loss per unit volume will increase as the flux density increases. However, it is not clear whether the total core loss will increase or decrease and a calculation of the total loss is needed to see the net result. Another issue to note here is the fact that the saturation flux density levels given in Table 2.2 are for room temperature (25°C). In fact, the saturation flux density drops to about **0.5 T** for the Square Permalloy and the Supermalloy alloys at **200°C** (according to Magnetics). This information was obtained by consulting one of the applications engineers at Magnetics. As a result, an operating flux density level is picked as **0.4 T** to carry out the transformer design. This represents the upper limit for the materials investigated since higher flux densities may result in core saturation at the specified operating temperature.

Specifying the number of turns affects the transformer design as discussed earlier in chapter 1. From the proposed transformer specifications, a split secondary is needed with the ability to double the input voltage. Hence, a 1:2 primary to secondary turns ratio is needed. Increasing the primary number of turns tends to reduce the required core cross sectional area by the same factor if everything else is fixed. As a result, the core size will go down and the total core loss will decrease. However, the copper loss will increase accordingly. In this application, and since the core loss is expected to be larger than the copper loss, increasing the

number will have the net result of reducing the total losses. Since the outer winding is a copper tube, and multi turn construction in the lab is rather troublesome for more than two turns, the primary turns were picked to be **two turns**. As a result, the secondary will have **four turns**.

At this point, the final proposed transformer specifications are as follows:

Base Plate Temp.	: **200°C**,	Power Rating	: **2.5 kVA**
Frequency	: **20 kHz**,	Prim. Voltage Rating	: **125 V rms**
Primary Turns	: **2 turns**,	Sececondary Turns	: **4 turns**
Prim. Current Density, J_p	: **600 A/cm^2**,	Sec. Current Density, J_S	: **400 A/cm^2**

(Note: The typical current densities used in designing CWT are higher compared with the conventional design since the aforementioned one has a larger winding surface area)

The transformer first pass design steps are summarized as follows:

1) From the specified kVA, the secondary rms current can be computed to be **10 A rms.** Hence, the secondary winding wire area needed, A_{wire} is computed as,

$$A_{wire} = \frac{I_S}{J_S} = 0.025 \text{ cm}^2 = 4934 \text{ cir mils} \qquad (2.1)$$

Selecting a copper wire with a cross sectional are > 4934 cir mils results in AWG 12 wire (see appendix B). For a stranded AWG 12 wire, the outer diameter is approximately 3.0 mm.

2) Since the secondary turns are 4, the equivalent inner winding radius r_i is compute as (refer to Fig. 2.1),

$$r_i = \left(1+\sqrt{2}\right)\frac{OD}{2} = 0.3621 \text{ cm} \qquad (2.2)$$

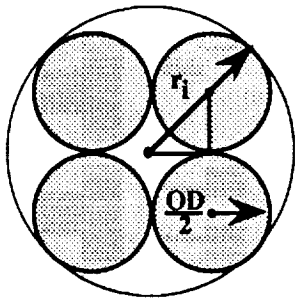

Fig. 2.1 Computation of r_i for a four turn inner winding

3) Once r_i is specified, an outer tube can be selected which fits over the inner winding. Since the ratio of the outer tube inner radius r_{ti} to the inner winding radius r_i affects the leakage inductance, minimizing this ratio will minimize the leakage inductance. A ratio of 1.75 is picked to allow for enough window area to wind the inner winding. Hence,

$$r_{ti} = 1.75\, r_i = 0.6336 \text{ cm} \tag{2.3}$$

4) Given the primary current density, the outer tube cross sectional area can be computed to as,

$$A_{tube} = \frac{I_p}{J_p} = \frac{\pi}{N_p}(r_{to}^2 - r_{ti}^2) = \frac{20}{600} = 0.0333 \text{ cm}^2 \tag{2.4}$$

Hence, the outer tube outer radius needed is,

$$r_{to} = \sqrt{\frac{N_p}{\pi} A_{tube} + r_{ti}^2} = 0.65 \text{ cm} \tag{2.5}$$

and the copper tube thickness is computed to be,

$$\Delta t_{tube} = r_{to} - r_{ti} = 0.0164 \text{ cm} \tag{2.6}$$

Since the operating frequency is 20 kHz, the skin δ depth is computed for copper at 20 kHz as,

$$\delta = \sqrt{\frac{\rho}{\mu_o \pi f}} = 0.051 \text{ cm} \tag{2.7}$$

where ρ is resistivity of copper (0.205×10^{-7}). Note here that the estimated copper tube thickness Δt_{tube}, is significantly less than the skin depth δ. A significantly lower ac resistance can be attained by increasing the tube thickness (which reduces the current density). As a matter of fact, it was shown by Rauls [4] that a copper tube thickness of 1.57δ provides minimum ac resistance. Using the 1.57δ as the copper tube thickness, r_{to} is recalculated as,

$$r_{to} = r_{ti} + 1.57\delta = 0.7136 \text{ cm} \tag{2.8}$$

Hence, the outer tube outer diameter is 1.427 cm or 0.562 in.

5) Once the tube is specified, a core can be selected that fits over the specified copper tube. Notice here that the core inner diameter should be larger than the outer diameter of the copper tube to allow for some insulation between the outer tube and the core, i.e. greater than 0.562 in.

By surveying the available cores sizes in the MAGNETICS catalogue, the smallest core size that fits these specifications has an inner diameter of 0.6 in. The core selected for the first

pass design is MAGNETICS 53296, which is a 1 mil tape unboxed core. The core data is as follows:

ID	= 0.6 in,	OD	= 0.9 in,	HT	= 0.25 in
A_{core}	= 0.182 cm^2	l_m	= 5.98 cm		

6) Once a core size is picked, the total number of cores required is determined from the total core cross sectional area needed to support the applied voltage. From (1.7), A_C is computed via,

$$A_c = \frac{V_p}{4.44 f N_p B} = 17.595 \text{ cm}^2 \tag{2.9}$$

Note that B is in Teslas. Hence, the total number of cores N_C is computed as,

$$N_c = \frac{A_c}{A_{core}} = 96 \tag{2.10}$$

and the total core length is,

$$l_{core} = N_c \, HT = 24.0 \text{ in} \tag{2.11}$$

7) At this stage, all transformer dimensions are specified. The next step is to estimate transformer performance. This is done by estimating the copper and core loss of the transformer.

a) <u>Copper Loss:</u>

The copper loss for the inner and outer windings is calculated as,

$$P_{cu} = I_{rms}^2 R_{ac} \tag{2.12}$$

where the ac resistance per unit length is calculated for one skin depth thickness by,

$$R_{ac} = \frac{\rho}{\pi \left[r_{wo}^2 - (r_{wo} - \delta)^2 \right]} \quad \Omega/\text{m} \tag{2.13}$$

where r_{wo} is the conductor or tube outer radius, ρ is the copper resistivity. Note here that the outer winding resistance is two times the value given by (2.13) since the copper tube is split in half. Since the ambient temperature is 200°C, the net resistance will be higher than that computed at room temperature. To account for that, the total ac resistance per unit length is computed as,

$$R_{ac,T} = (1 + \alpha \Delta T) R_{ac} \tag{2.14}$$

where α is the temperature coefficient of resistance and ΔT is the temperature rise. For copper, α is 0.0039 at 20°C while ΔT is 180°C for 200°C operation.

b) Core Loss:

The core loss is calculated for the three materials previously selected in the previous section. In order to calculate the core loss, the core material core loss per unit volume for each material and the total core volume are needed. The core loss per unit volume is obtained from the manufacturer's catalogues at the specified frequency and flux density level.

An Excel spread sheet was used in order to evaluate the performance of the designed transformer and the results are shown in Table 2.3.

Table 2.3 Estimated transformer performance results using MAGNETICS 53296 core

Material	Metglas 2605 S3A	Square Permalloy	Supermalloy
Inner winding copper loss (W) @ 25°C	4.45	4.45	4.45
Outer winding copper loss (W) @ 25°C	0.917	0.917	0.917
Total core loss (W) @ 25°C	23.55	36.11	32.10
Inner winding weight (lb.)	0.408	0.408	0.408
Outer winding weight (lb.)	0.102	0.102	0.102
Core weight (lb.)	1.68	2.01	2.01
Total weight (lb.)	2.192	2.52	2.52
Total Losses (W)	28.65	41.21	37.19
Efficiency	98.84 %	98.34 %	98.50 %

It is clear from Table 2.3 that the dominant losses in this transformer are the core losses. Note here that the table includes the estimated weight data.

The total transformer length is computed by first computing the copper tube length as,

$$l_{tube} = l_{core} + \pi OD_{core} = 0.753 \text{ m} = 29.64 \text{ in} \quad (2.15)$$

Hence, the transformer length (assuming a U shape structure),

$$l_{transf} = \frac{l_{tube}}{2} = 14.82 \text{ in} \quad (2.16)$$

8) Finally, the transformer leakage and magnetizing inductances can be estimated using the formulas given in chapter one which result in,

$$L_{leak} = 487.86 \text{ nH}, \qquad L_{mag} = 7.3 \text{ mH } (@ \mu_r = 10{,}000)$$

2.3 Final Transformer Design

At this stage, a first pass design was obtained. Most of the obtained data are reasonable except for the total transformer length. An optimal transformer design can be attempted by following the iteration algorithm described earlier in chapter 1. Since the frequency is fixed and the flux density was chosen near its upper limit, and since the number of turns was chosen on the basis of manufacturability, the remaining things to adjust are the winding window area and the length to width ratio.

As discussed in chapter 1, decreasing the winding window area results in increasing the winding losses while decreasing the core losses. However, since the hottest spot in the transformer is expected to be the inner winding, an increase in the copper losses will result in higher temperature rise. In addition, the area available to wind the inner winding will become tighter. On the other hand, increasing the window area will result in higher core losses. As a result, it seems that the window area obtained from the first pass design is rather reasonable.

Concerning the length to width ratio, it was argued in chapter 1 that having a high length to width ratio tends to decrease the core losses, which are the dominant losses in this design. However, the resultant transformer will be rather long. Hence, a compromise is needed between the transformer core losses and the transformer length.

The transformer design and performance equations were written into an Excel spread

sheet and transformer designs for different core sizes were obtained for the previously specified core materials. The cores were picked from the MAGNETICS catalogue. These cores were selected based on the estimated outer diameter of the copper tube calculated in step 4 of the previous section which was **0.561** inches. In fact, an available copper tube that closely matches the calculated one is a **5/8" (0.625")** outer diameter, **28 mil** tube, which was obtained from manufacturer's data catalogues. Note here that the 1.57δ, which the thickness of minimum ac resistance introduced in step 4 of the previous section, is approximately **31 mil**. Since the outer diameter of the tube is 0.625 in, the selected core should have an inner diameter larger than 0.625 in order to allow for some insulation. Hence, the cores selected have an inner diameter of **0.75"** while the outer diameter is in the range of **1.0"** to **1.5"**. Figure 2.2 shows the projected efficiency for these transformers using the different core materials as a function of the core volume. In addition, the total core length as a function of the core volume is also shown in Fig. 2.2. The Excel output data are listed in appendix C.

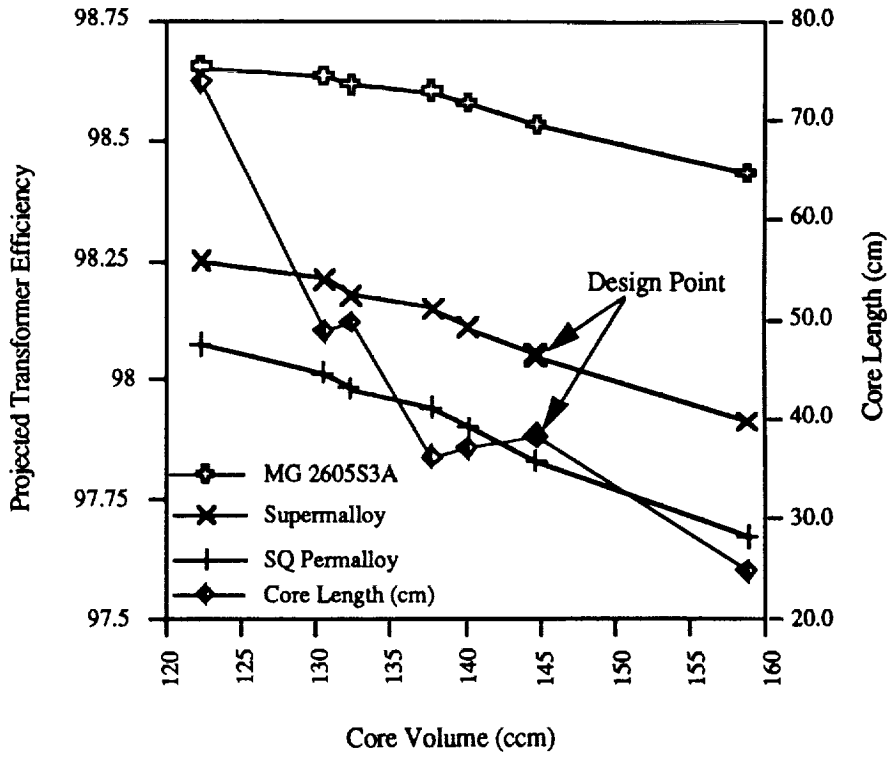

Fig 2.2 Projected transformer performance as a function of core volume @ 25°C with B = 0.4 T, f = 20 kHz, Np = 2, Ns = 4, 125 V rms input voltage

It is clear from Fig. 2.2 that the Metglas 2605 S3A material has the highest projected efficiency. However, since the data obtained for this material were obtained from the ALLIED SIGNAL catalogue, no readily manufactured cores were available. In addition, the curie temperature for the Metglas material is 358°C which less than that for the Square Permalloy and the Supermalloy. As a result, the Metglas material was excluded to allow for some safety factor in temperature rise. One last thing to note is that the performance of the transformer with the Supermalloy seems to be better than that with the Square Permalloy. As a result, the **Supermalloy** will be the core material of choice for this project.

The final step is to select the core size that will be used for the final design. As shown in Fig. 2.2, as the core volume decreases, the core length increases and the transformer efficiency improves. This is expected since, as discussed in chapter 1, the core loss can be minimized by making the length to width ratio as high as possible . Hence, it is reasonable to pick the core with the highest efficiency. However, the core length will be large for such a design (**70 cm**). A compromise between the transformer efficiency and the transformer length can be made based on the transformer specifications. Since there are no specifications for the transformer length, the selected core corresponds to the design point shown in Fig. 2.2. Even though the projected efficiency for this design is not maximum, the total transformer length is almost minimal. The core material is Supermalloy with 1 mil alloy thickness. This design corresponds to the core number 53481 with the following data (MAGNETICS catalogue),

ID = 0.75 in, OD = 1.25 in, HT = 0.5 in

A_{core} = 0.605 in, l_m = 7.98 cm

The expected transformer data, as calculated by Excel are listed in Table 2.4.

2.6 Insulation Materials and Transformer Assembly

As discussed earlier in chapter 1, one of the basic considerations is a high temperature insulation material (> 200°C). In this section, the different insulation materials used in

addition to the transformer assembly will be discussed.

For the inner winding, a stranded AWG 12 copper wire was ordered from Omega Inc. It has an insulating material of fiber glass and ceramics and an operating temperature specification of 450°C, which is adequate for this application. The total wire length as specified in Table 2.4 is 7.62 ft. The inner winding was wound after the transformer was constructed.

Table 2.4 Projected transformer data using the 53481 Magnetics core

Parameter	Expected Value
Flux Density (B)	0.4 T
Cross Sectional Area (A_c)	18.15 cm^2
Frequency	20 kHz
Number of Turns	Np = 2, Ns = 4, split sec.
Core Loss (P_c)	44.5 W @ 25°C
Copper Loss (P_{cu})	4.14 W @ 10 A rms, 220°C 9.31 W @ 15 A rms, 220°C
Efficiency	98.05 % @ 2.5 kVA
kVA Rating	2.5 kVA
Temperature Rise in °C	52.8°C (For Core)
Number of Cores	30
Core Length	15 in
Weight	3.17 lb (Epoxy not included)
Length	10.75 in
Width	3.13 in
Secondary Wire Total Length	2.322 m or 7.62 ft
L_{leak} (prim. referred)	376 nH
L_{mag}	14.72 mH
Relative Permeability (μ_r)	30,000

The primary winding, which is a two turn winding, consists of a U-shaped copper tube cut in half. The construction of the primary winding was accomplished by first cutting the

copper tube into two halves along a radial axis. Since the total core length is 15 in, or 7.5 in if the transformer is folded into a U shape, the required total tube length should be larger than 7.5 inches in order to allow for soldering turn interconnections at both the front and back ends. As a result, the required tube length is in the order of 9.0 inches. The back ends of the copper tube halves were cut at 45° angles and then soldered by brazing with another two smaller halves cut at 45° angles to form the U-shape as shown in Fig. 2.3.

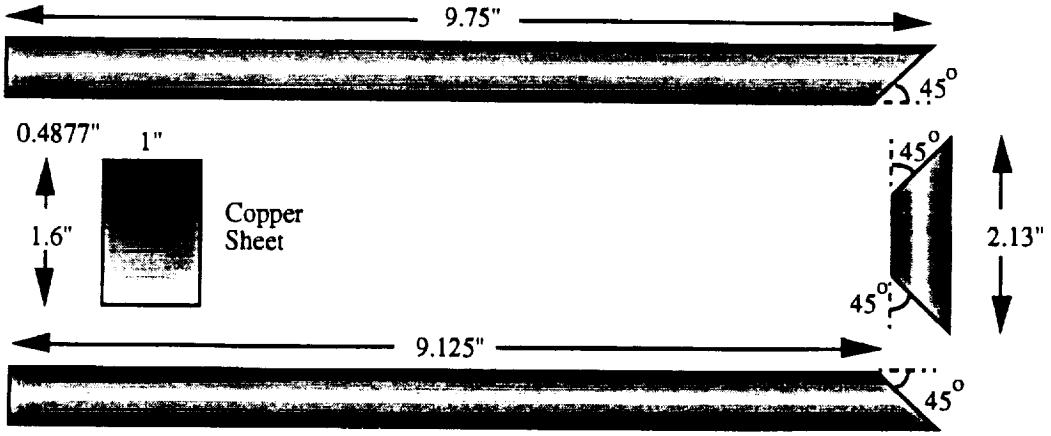

Fig. 2.3 Primary winding construction

Note in Fig. 2.3 that the upper half on one side and the lower of the other half are longer by about 0.5 inches to allow for primary winding connections with the power converter. A copper sheet was soldered at the front end of the tube halves to connect one half with the other as shown in Fig. 2.4.

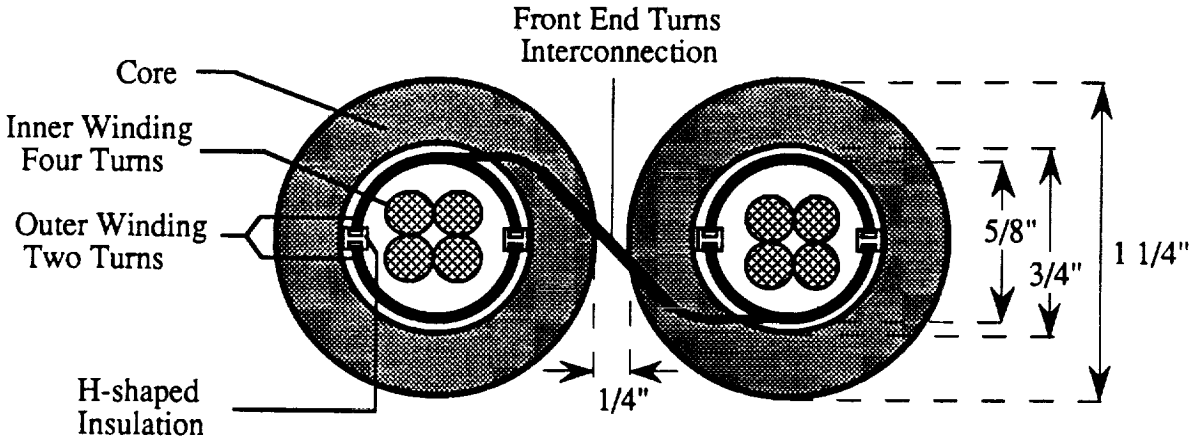

Fig. 2.4 Cross section of the transformer front end

Since the primary tube consists of two halves, insulation is needed between the two halves. In addition, the insulating material should provide some sort of support for the two halves to hold them together. For this purpose, a Fluorosint 500 insulating rod of 0.5 inch diameter was selected and ordered from Cadillac Plastic and Chemicals Co.. The temperature specification for this material is 650°F (343°C). The rod was machined into an H-shaped block to provide the necessary insulation and support. The two halves were mounted on both sides of the H-shaped block as shown in Fig. 2.5.

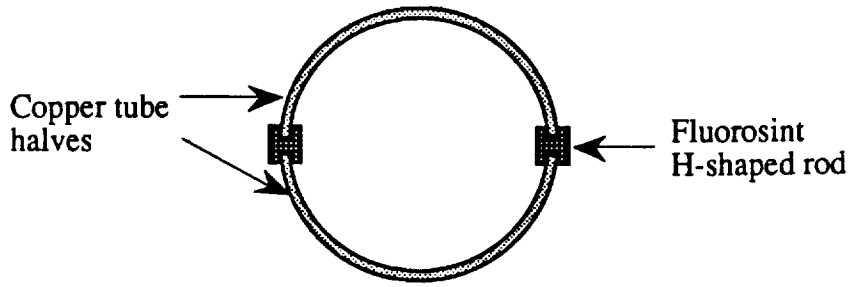

Fig. 2.5 Insulating the tube halves using an H-shaped rod

The core is insulated from the outer winding using a 5 mil, two layer Kapton sheet. The temperature specifications for Kapton are approximately 250°C. Insulation between the core ends and the tube is provided using Mica rings of an inner diameter of 0.75 in. The temperature specifications for Mica are in excess of 300°C. The Final transformer layout is shown in Fig. 2.6. A summary of the designed transformer components with some of their specifications is given in Table 2.5.

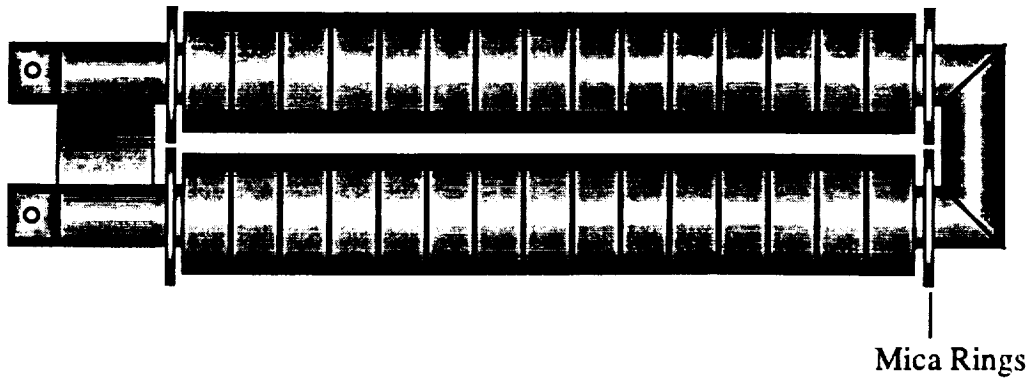

Fig. 2.6 Designed transformer layout

Table 2.5 Designed transformer components

Component	Material Used
Magnetic Core Material Selected	Tape wound Supermalloy 1 mil Curie Temp.: 400°C (Magnetics)
Core Selected	53481 from Magnetics Catalog ID=0.75", OD=1.25", HT=0.5", Ac=0.605 cm^2
Primary Conductor	Two halves of copper tube of 5/8" diameter, 28 mil thickness
Core and Tube Insulation	Two sheets of 5 mil Kapton Mica rings at both core ends
Secondary Wire	Stranded copper wire, AWG 12 Insulation: fiber glass and ceramics, 450°C

2.7 Conclusions

In this chapter, the design methodology used in meeting the proposed specifications were presented and discussed. The final transformer design was constructed in the lab.

In the next chapter, the designed transformer will be tested and experimental results will be obtained. A comparison between the expected and experimental results will finally be made,

Chapter 3

TRANSFORMER TESTING AND EXPERIMENTAL RESULTS

3.1 Introduction

The key point in testing transformers is to identify the loss components in addition to the parameters needed to construct an equivalent circuit, namely, the leakage and magnetizing inductances and the core and copper loss resistances. The equivalent circuit model for the co-axial winding transformer, as derived earlier in chapter 1, is shown in Fig. 3.1.

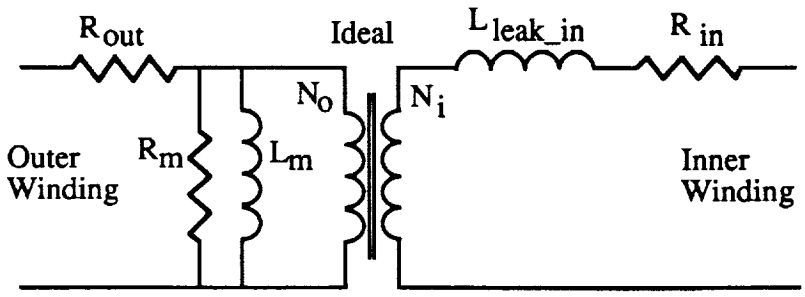

Figure. 3.1 Equivalent circuit model for the two winding co-axial transformer

In this chapter, the experimental transformer will be tested and the measured data will be compared with the expected data. The test setups used will be explained and shown accordingly.

3.2 Test Setups

This section will describe the test bench setup in addition to the equipment used to carry on the tests.

The test setups are as follows:

1) Input Excitation:

A full bridge inverter, shown in Fig. 3.2, was used to provide the required excitation to the transformer. Hence, the input excitation was a square wave rather than a sine wave.

However, core losses will not be affected if the transformer is excited at the same flux density level as that of a sine wave. Since the input is a square wave, the peak voltage needed to establish a 0.4 T flux level is 116 V (compared to 125 V rms sine input). Note here that the actual cross sectional area of the selected core is **18.15** cm^2.. For measuring copper loss, the transformer was excited with rated rms current with the other winding short circuited.

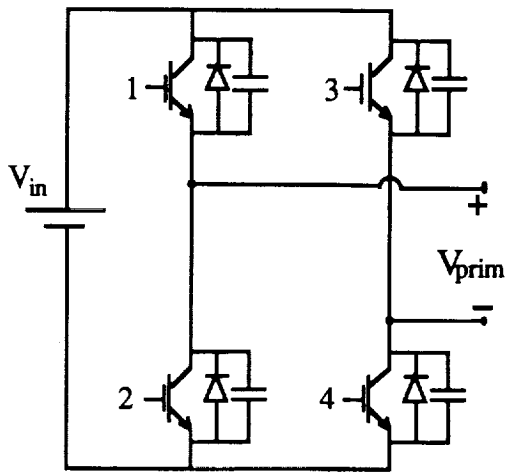

Fig. 3.2 Full bridge inverter for square wave excitation (f=20 kHz)

2) High Temperature Compartment:

A household oven was used to provide the required high temperature environment for testing. A small fan was installed in the bottom of the oven to assure even distribution of temperature inside the oven when it is operating. A hole was drilled on one side of the oven to interconnect the transformer leads with the outer circuitry. A sketch of the oven system is shown in Fig. 3.3. Note here that a 1/8" **Ceramic** board (ordered from Cotronics Corp. [10]) was used to insulate the tested transformer from the oven rack. Another ceramic board was used in the bottom of the oven, just above the fan, to prevent any air flow from the fan on the transformer. The temperature specification for the ceramic board is 3000°C.

3) Temperature Measurement:

In order to measure temperature, four thermocouples were mounted on the transformer as shown in Fig. 3.3. The thermocouple type used is a **Code T** 350°C ordered from

Omega [11]. The thermocouples were mounted on the transformer using a high temperature epoxy. The epoxy used is an EPOX EE 4700 ultra temperature ordered from Cotronics Corp [10]. The process of applying the epoxy involved curing the transformer after the epoxy was applied at different temperatures for four hour intervals. The temperature was measured using an Omega, Type T Thermocouple Thermometer.

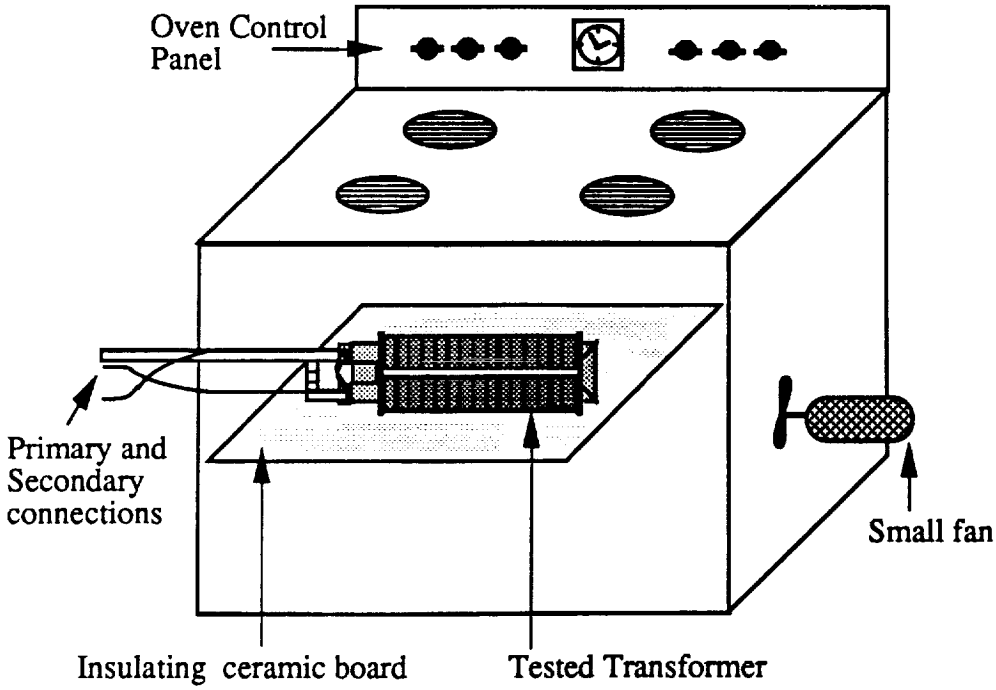

Fig. 3.2 Oven setup

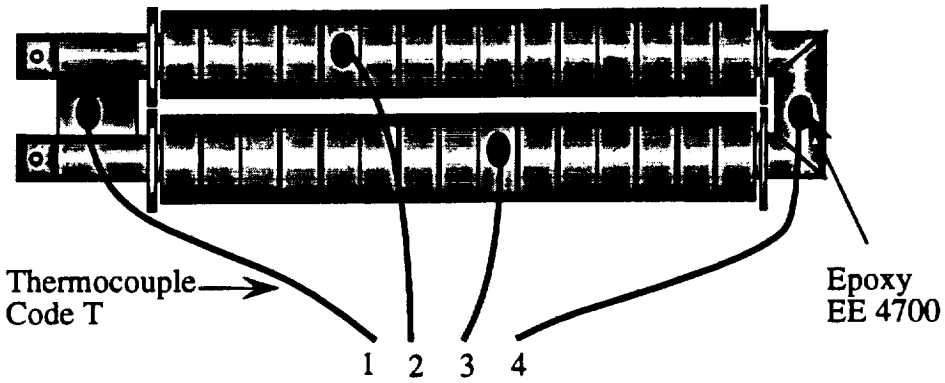

Fig. 3.3 Thermocouple mounting

4) Equipment used:

The equipment used in testing the transformer includes two ISOBE isolators for voltage measurement, two current probes and amplifiers for current measurement in addition to a four channel LeCroy scope. The LeCroy scope has a storage capability and was also used to compute the rms value of the current wave form in addition to the input/output energy for the transformer. Figure 3.4 shows a block diagram of the whole testing system.

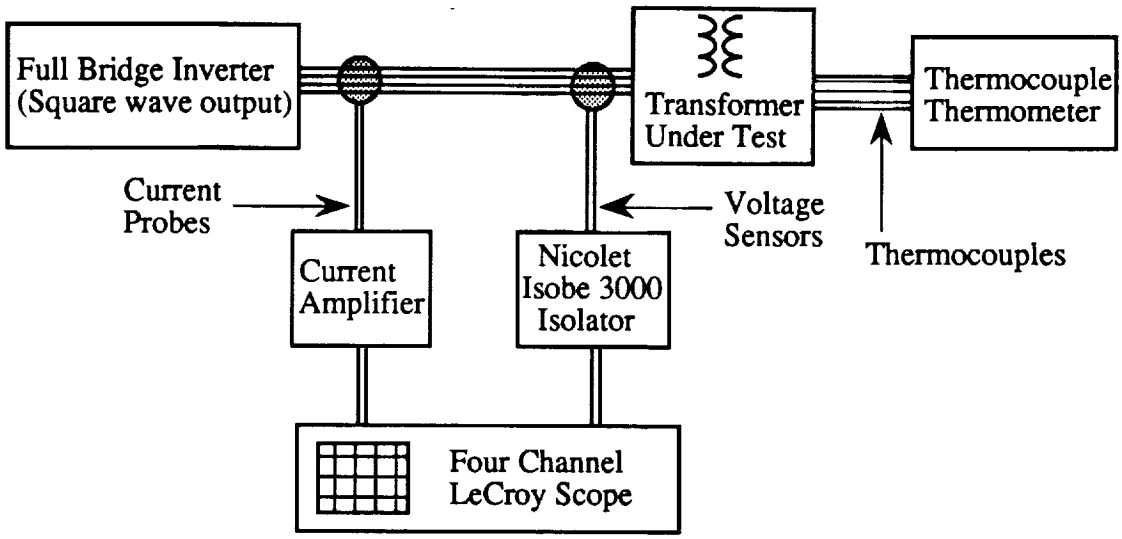

Fig. 3.4 Block diagram of the system test setup

3.3 Testing and Experimental Results

As noted earlier, the aim of testing is to identify the transformer loss components, namely, core and copper loss, in addition to measuring the transformer magnetizing and leakage inductances. Once these parameters are identified, the transformer model can be obtained.

In this section, the test procedure used to obtain the parameters of interest will be presented in addition to the test results. Finally, a summary of the test result data will be presented. Throughout the testing, the outer winding (tube) is referred to as the primary winding, while the inner winding is referred to as the secondary winding.

3.3.1 Core Loss and Magnetizing Inductance Measurements

Conventionally, the core loss of the transformer is measured by what is called the open circuit test. The primary of the transformer is excited with rated input voltage while the secondary winding is left open. As a result the rated flux is established in the core and the only current that flows is the magnetizing current.

Since the secondary winding is left open, the only significant loss component is the core loss which is determined by measuring the input power at the transformer terminals. This is done by inserting voltage sensing wires at the transformer terminals to measure the voltage across the transformer, while the input current is measured with the current probe. Displaying these signals on the scope shows the primary voltage and the magnetizing current.

Since the flux is the integration of voltage, the flux signal can be obtained by integrating the voltage across the transformer. Another way is to connect an RC circuit across the primary winding. The R and C are selected so that the maximum current in the RC circuit is only 1 % of the magnetizing current. In addition, the resistance value should be at least 100 times larger than the capacitive impedance. This guarantees that the current in the RC circuit is basically determined by the resistance only. As a result, the current signal will be proportional to the primary voltage. Since the capacitor voltage is the integral of the current, which is in turn proportional to the input voltage, the capacitor voltage will be proportional to the flux in the core. The R and C were computed based on the previous constraints as 31 kΩ and 0.0255 μF. The values used were 32 kΩ and 0.047 μF. The test circuit is shown in Fig. 3.5.

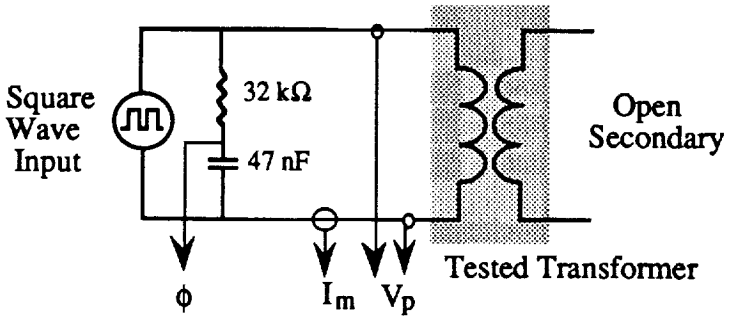

Fig. 3.5 Open circuit test circuitry

The input voltage is generated, as discussed earlier, by an inverter bridge circuit. In order to have a flux density of 0.4 T in the core, the square wave input to the transformer needs to be 116 volts (which is the same as the rms). Note that the difference in the applied voltage compared with a 125 rms sine wave is the wave factor, which is 1.11 for sine wave and 1.0 for square wave.

The B-H curve shape can be investigated by displaying the flux signal versus the magnetizing current signal. This is due to the fact that the magnetic field intensity is proportional to the current in the circuit.

Before running the open circuit test, the oven was turned on and set for 200°C temperature and left for half an hour until the temperature stabilized. Then, the transformer was excited with a 20 kHz, 116 volts square wave input. The flux and current signals in addition to the B-H loop are shown in Fig. 3.6. The core loss is measured directly on the scope. This is done by multiplying the current and voltage signals then integrating the product. The resultant signal is the lost energy E_{in}. By taking the difference in energy over one cycle and dividing that by the period of the cycle (50 μs), the average core loss power is measured. Figure 3.7 shows the magnetizing current, the flux and the transformer voltage in addition to the resultant energy signal. As shown in this figure, the difference in energy over five cycles is 1.344 $\mu V^2 s$. By first multiplying this number by the gain settings of the Isobe and the current amplifier and then dividing it by the time difference, the resulting core loss is **26.88 W**.

Core loss measurements were taken at different temperatures, namely, 25°, 100°, 150° in addition to 200°C. The measured core losses, using the procedure just described above, were 35 W at 25°C, 30 W at 100°C, 28 W at 150°C and 27 W at 200°C. These results are plotted in Fig. 3.8. Since eddy current losses are inversely proportional to the core resistivity and due to the fact that the core resistivity increases as the temperature increases, eddy current losses will decrease. For hysteresis losses, it was shown by Fritz and Clark [12] that both the saturation induction and the coercivity decrease with increasing temperature (appendix D). As a result, the hysteresis loop will get smaller and hence, the hysteresis loss will decrease.

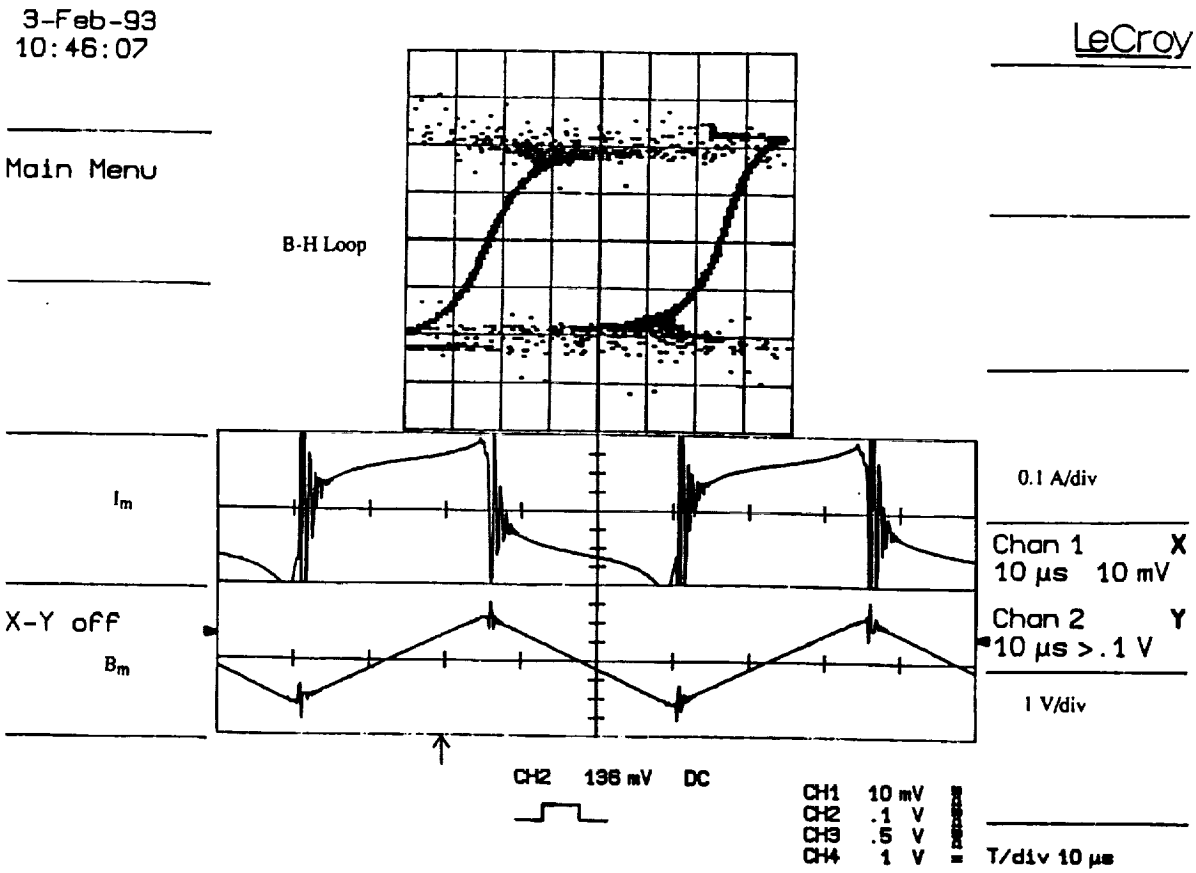

Fig. 3.6 Open circuit test results at 200°C, 20 kHz and 116 V square wave input

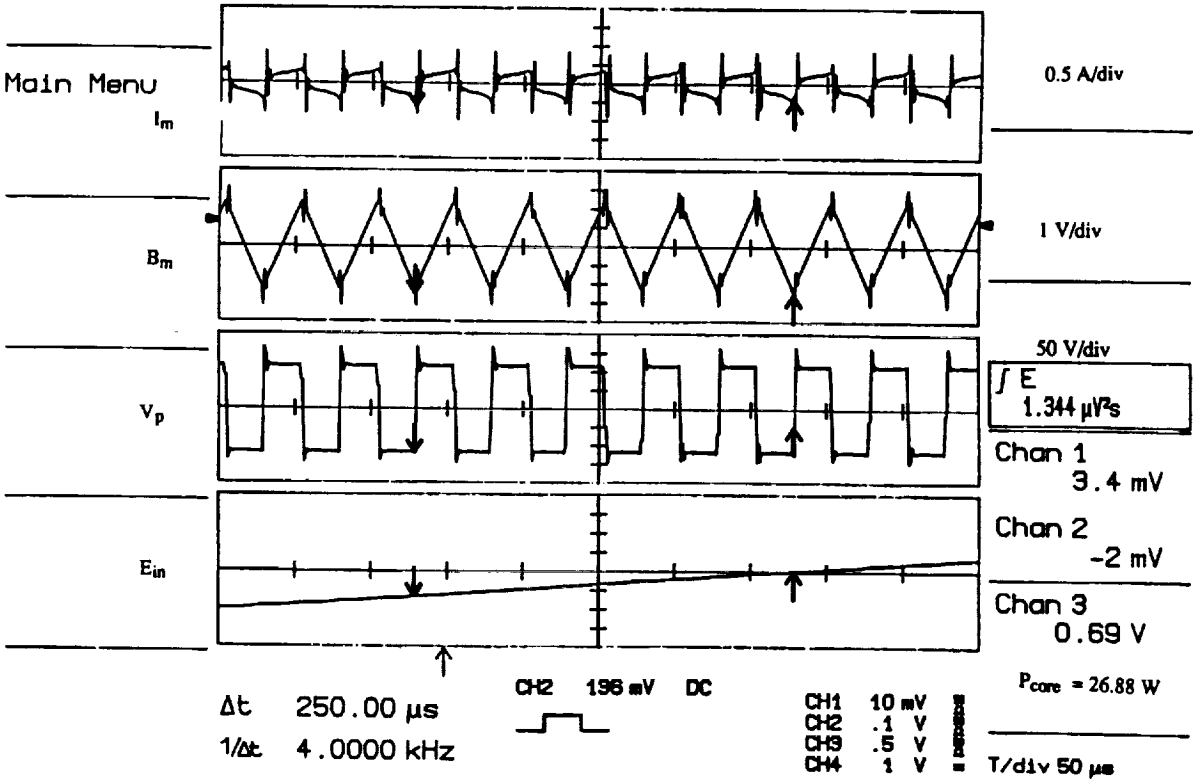

Fig. 3.7 Open circuit test results showing core loss measurement

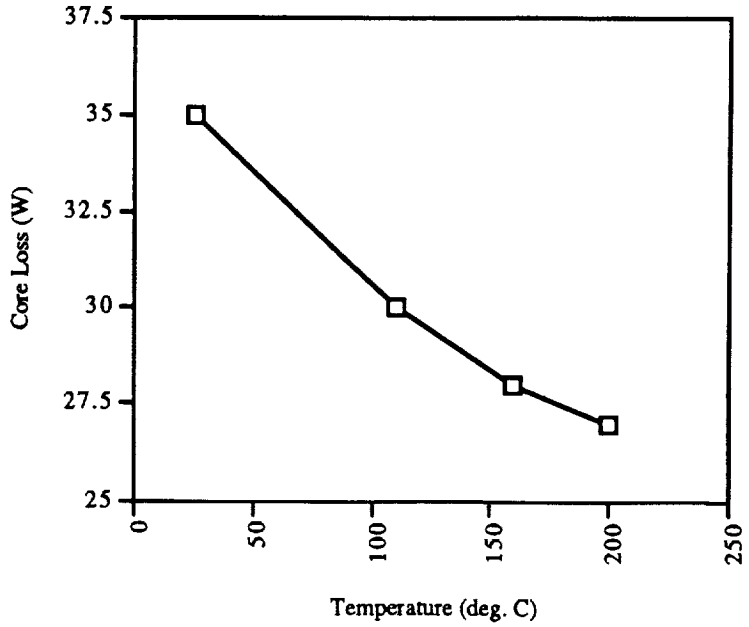

Fig. 3.8 Core loss data versus temperature

The core loss resistance can be estimated as,

$$R_m = \frac{V_{in}^2}{P_{in}} = 498\ \Omega \tag{3.1}$$

The magnetizing inductance, L_m, can be measured by measuring the slope of the magnetizing current from Fig. 3.7. In fact, by investigating Fig. 3.7, the magnetizing current doesn't have a linear rise or fall but rather a close to exponential shape. This is due to the fact that the effective core loss resistance value is comparable with the magnetizing impedance. Nevertheless, by estimating the average slope of the magnetizing current (using the digital scope), the magnetizing inductance is found as,

$$L_m = \frac{V_{in}}{\Delta I/\Delta T} = \frac{116}{0.182/18.675\text{x}10^{-6}} = 12.0\ \text{mH} \tag{3.2}$$

Hence, the magnetizing reactance,

$$X_m = 2\pi f L_m = 220\ \Omega \tag{3.3}$$

1.3.2 Copper Loss and Leakage Inductance Measurements

The conventional method for measuring the copper loss is the short circuit test. One pair of the transformer terminals is short circuited while the other terminal pair is excited with

the rated current. Since one winding is shorted, very little flux will be established in the core, and the only loss component is the copper loss. This test also can be used to measure the leakage inductance of the transformer.

One problem with the short circuit test stems from the name of the test itself. Since one of the transformer windings is shorted, a very small input voltage to the other winding results in a large current in the transformer. Hence, it is not easy to control the input voltage to provide the necessary rated current. One way to solve this problem is to connect a large inductance in series with the test winding (the unshorted one). The large inductance serves as a current limiting impedance (current source) and provides a linear rise or fall of current for a square wave input. On the other hand, the voltage needed to establish the rated current in the transformer is rather high and hence easy to control. Since the transformer rating is 2.5 kVA with 125 V rms input voltage, the primary rms current is 20 A while the secondary rms current is 10 A.

Since either of the transformer terminals can be shorted for copper loss measurement, it was chosen for this test to short the primary winding and apply the excitation to the secondary winding. This is done to facilitate the measurement of the leakage inductance. By referring to Fig. 3.1, it was shown that the leakage inductance in a co-axial winding transformer is only present on the secondary side (inner winding). Since the primary to secondary turns ratio is 1:2, the primary referred leakage inductance will be one fourth the secondary leakage. Hence, the value of the leakage on the secondary side is four times larger than that on the primary side, and hence easier to measure.

In order to measure the leakage inductance the voltage across the secondary winding terminals is measured and divided by the slope of the input current. Voltage sensing wires were connected to the secondary winding at the transformer terminals to provide a good voltage signal. In order to obtain reasonable leakage inductance measurement, the copper loss impedance should be smaller than the leakage impedance so the voltage drop will be mainly due the leakage inductance drop.

The short circuit test circuitry is shown in Fig. 3.9. The value of the smoothing inductance used in this test was nearly 50 μH. Again here, the oven was first turned on for about half an hour until the temperature settled at 200°C, then the secondary winding was excited by the inverter bridge. The rated secondary rms current is 10 A which was verified by computing the rms value of the measured current signal on the LeCroy. The voltage that was needed to establish the rated current was nearly an 80 volt square wave input.

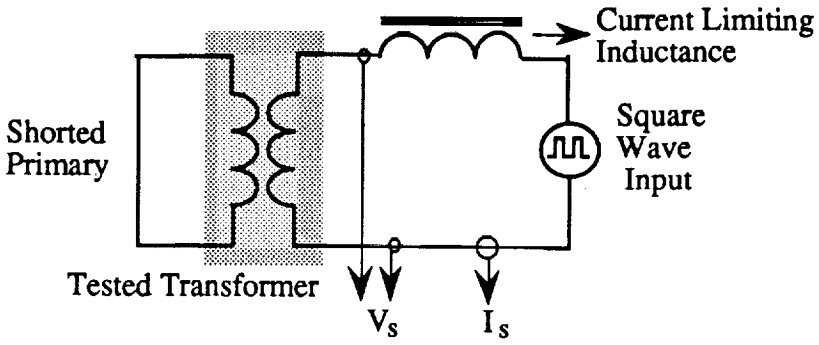

Fig. 3.9 Short circuit test circuitry

Figure 3.10 shows the secondary current and the voltage across the transformer secondary terminals. Note here that if the copper resistance was very small, the voltage across the secondary will be the derivative of the current and will be expected to be a square wave. However, the voltage here has a more nearly exponential rise due to the comparable copper resistance. The leakage inductance can be estimated by measuring the average peak positive or negative voltage and dividing that by the slope of the current. By doing so, the leakage inductance is found as,

$$L_{lk} = \frac{V_t}{\Delta I/\Delta T} = \frac{2.62}{18/11.09\text{x}10^{-6}} = 1.614\ \mu\text{H} \qquad (3.4)$$

By dividing L_{lk} by the square of the turns ratio, the primary referred leakage inductance is,

$$L_{lk\_p} = \left(N_s/N_p\right)^2 L_{lk} = 403\ \text{nH} \qquad (3.5)$$

The copper loss was measured in the same way the core loss was measured. The input current and voltage signals are multiplied and then the product is integrated. The resultant signal is the lost energy E_{in}. By taking the energy difference over a cycle and dividing it by the

period of the input signal (50 μs), the copper loss can be obtained. The resulting current, voltage and energy signals are shown in Fig. 3.11. From this figure, the energy difference over five cycles is 446 nV^2s. By first multiplying this number by the ISOBE and the current amplifier gains then dividing it by the time difference, the average power loss can be found. For this case, the average copper power loss is computed as **9 W**. Note that this copper loss data corresponds to the copper loss at the rated conditions, namely **2.5 kVA**. The total secondary referred copper loss resistance at 2.5 kVA can be estimated by,

$$R_{cu} = \frac{P_{in}}{I_{rms}^2} = \frac{9}{100} = 90\ m\Omega \tag{3.6}$$

The copper loss resistance can also be computed by referring to Fig. 3.10 as,

$$R_{cu} = \frac{\Delta V_R}{I_{p-p}} = \frac{1.9}{35} = 54\ m\Omega \tag{3.7}$$

Hence, the total copper loss is,

$$P_{cu} = R_{cu} I_{rms}^2 = 0.054 \times 10^2 = 5.4\ W \tag{3.8}$$

which is closer to what is expected. Note here that the energy method used to estimate the copper losses is very sensitive to dc offsets in the ISOBE isolator and the current amplifier since any dc offset is integrated and may result in measurement errors. On the other hand, the energy signal obtained from the scope contains an additional energy component caused by the high frequency oscillations in the voltage wave form which can not be isolated.

Another measurement was made for a **3.5 kVA** operation for the same voltage and an rms secondary current of 15 A. The measured copper losses were **21W**.

3.4 Temperature Rise Results

The transformer was tested at full load conditions by connecting a variable resistive load across the secondary winding while the exciting the primary winding with rated kVA (2.5 kVA). The input voltage was adjusted until the primary terminal voltage was at 116 volts which is the theoretical voltage needed to establish 0.4 T in the core. The resistive load was varied until a nominal 21 A rms current was measured in the primary circuit. The input kVA was obtained by multiplying the rms input voltage with the rms current which was 2.458 kVA.

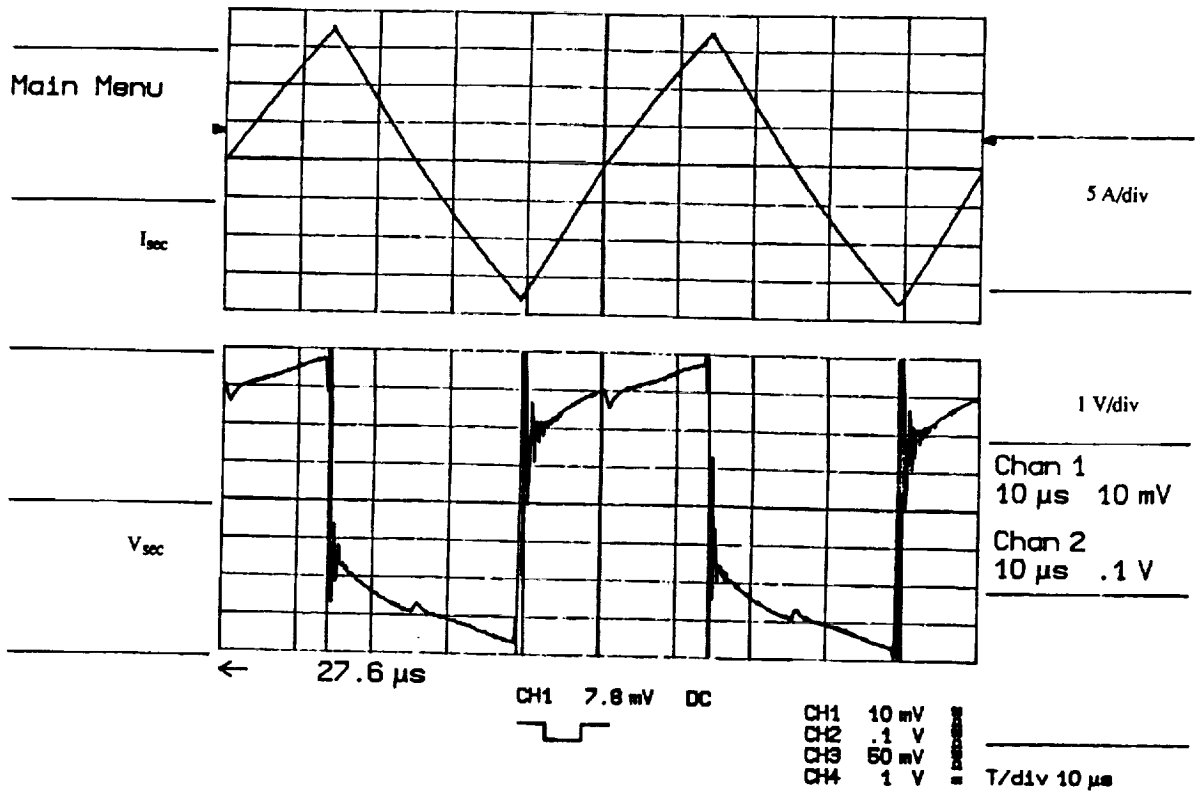

Fig. 3.10 Short circuit test results at 200°C and 20 kHz

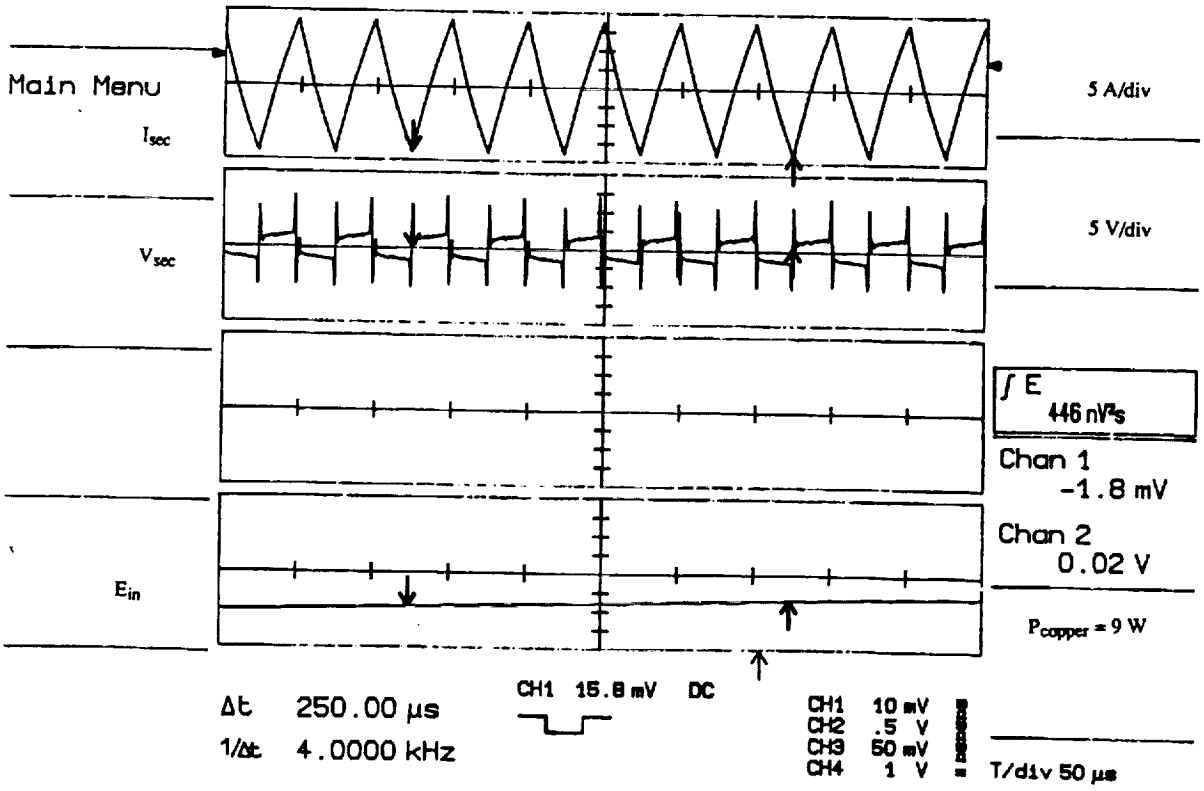

Fig. 3.11 Short circuit test results showing copper loss measurement

The output power across the secondary of the transformer was measured in the same way the core and copper losses were measured, namely, using the LeCroy. By doing so, the output power was measured to be 2.34 kW. The difference between the kVA and the kW readings is due to the fact that the load is not purely resistive but has an inductive component.

The transformer was tested at rated kVA for one hour, and the temperature readings obtained from the thermocouples were recorded. The thermocouples were mounted as shown earlier in Fig. 3.3. Figure 3.12 shows the temperature rise measurements of the thermocouples over a 60 minute span.

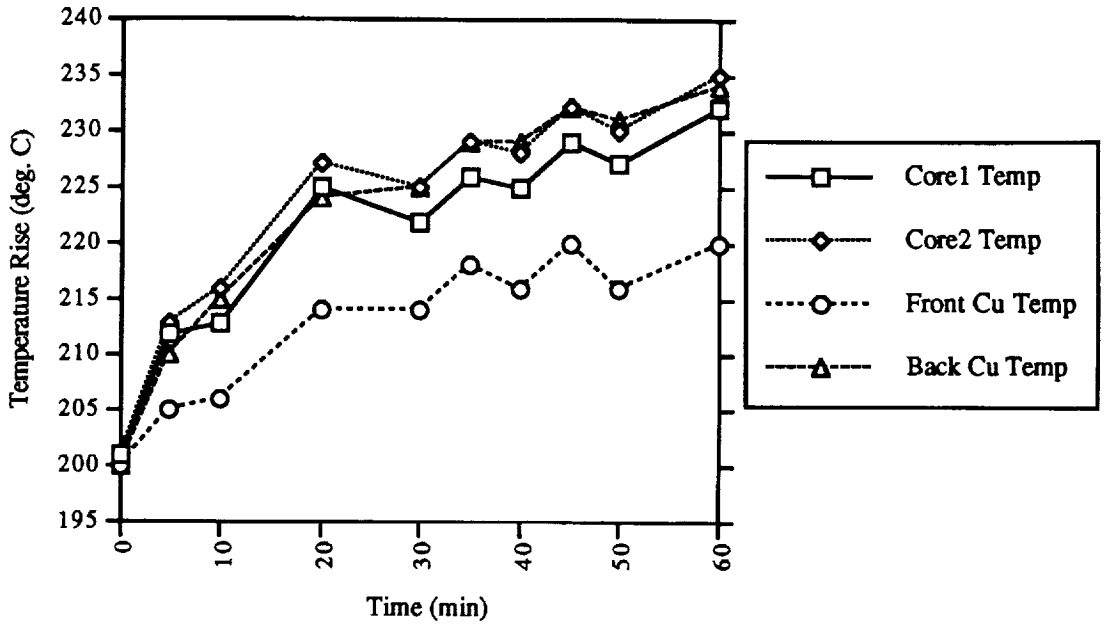

Fig. 3.12 Temperature rise measurements at 200°C ambient and 2.45 kVA

As shown in Fig. 3.12, the maximum recorded temperature rise was only 35°C although the temperatures may not totally have reached steady state. The voltage and current wave forms measured are shown in Fig. 3.13.

The transformer was also tested at 3.5 kVA load for one hour. The input voltage was the same as before while the rms current was increased by decreasing the load resistance. The input kVA to the transformer was 3.43 kVA while the output power was 3.22 kW. Again here, the difference between the kVA and the kW readings is due to the fact that the load is not

purely resistive. The temperature rise measurements over a 60 minute time span were recorded and are shown in Fig. 3.14. The maximum temperature on core or copper after one hour was 47°C. Figure 3.15 shows the measured current and voltage wave forms.

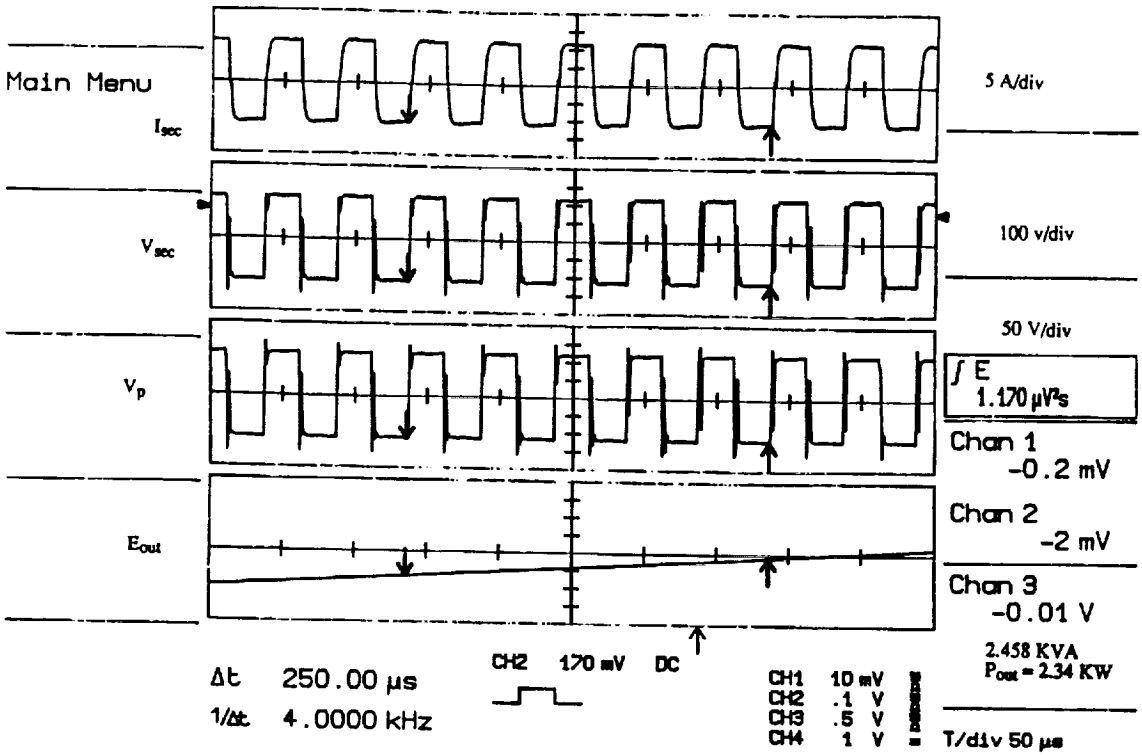

Fig. 3.13 Full load test results at 200°C and 2.45 kVA

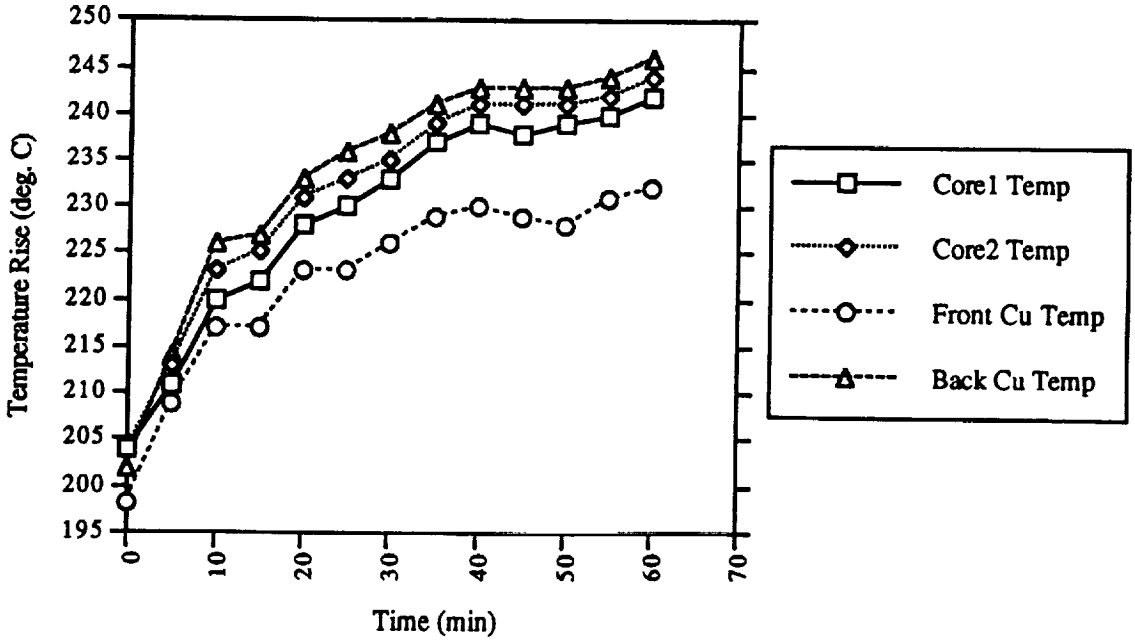

Fig. 3.14 Temperature rise measurements at 200°C ambient and 3.43 kVA

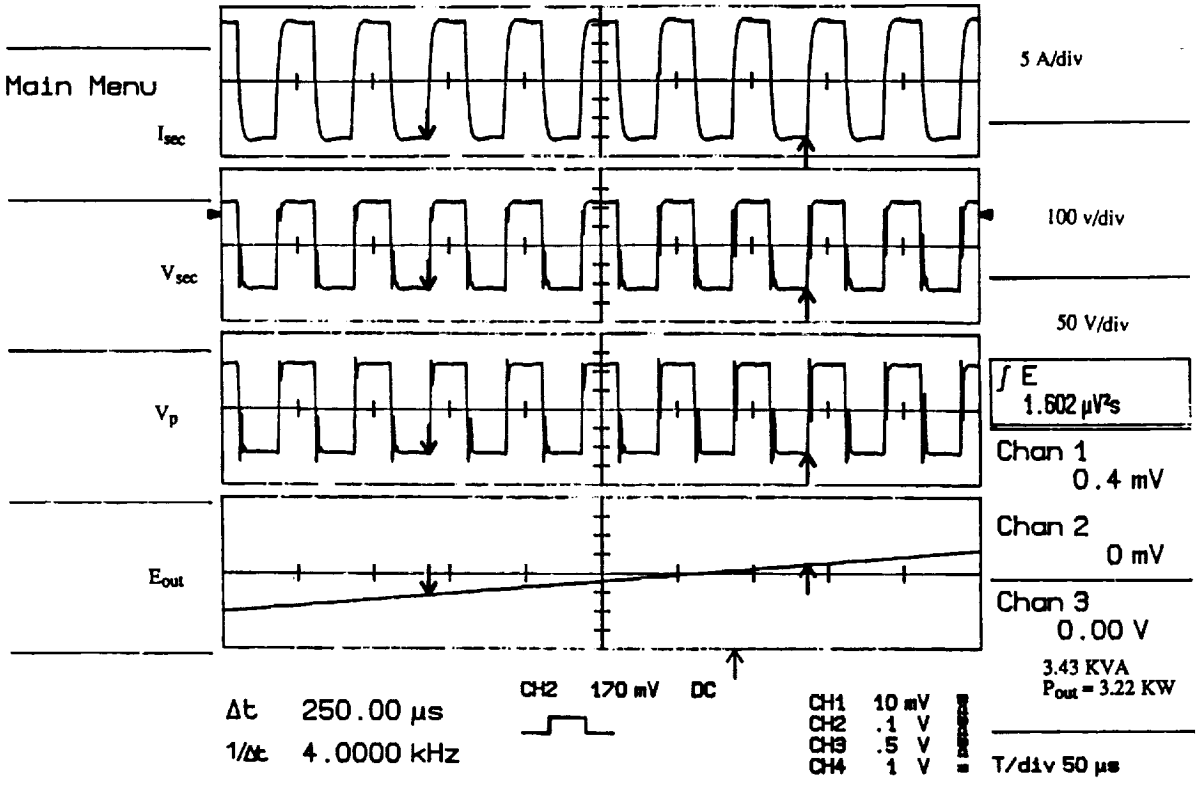

Fig. 3.15 Full load test results at 200°C and 3.43 kVA

3.5 Summary of Results

A summary of experimental results in addition to expected results is given in Table 3.1. Note here that all the measurements were done using square wave input excitation. This should not be significantly different than the sine wave excitation since the transformer was tested for the same rated flux and current levels.

By examining Table 3.1, the expected core losses are higher than the measured ones. The reason for that seems to be that the cores received from Magnetics were slightly larger than their specifications in the catalogue. This may be due to the special order of unboxed cores. In fact, when the weight of one core was measured, it was found to be 0.11 lbs compared to 0.09266 lbs specified in the catalogue. Hence, the total cross sectional area of the core is larger than what is expected. As a result, the flux density level in the core is less than 0.4 T which in turns means that the core loss per unit volume is lower.

Another issue to note is that the copper losses measured were higher than expected. As discussed earlier, this may be due to the effect of additional harmonic losses caused by the current wave form and additional skin effect or due to measurement error.

Table 3.1 A summary of expected and experimental results

Parameter	Expected	Measured
Flux Density , B	0.4 T	< 0.4 T
Cross Sectional Area, A_c	18.15 cm^2	> 18.15 cm^2
Frequency	20 kHz	20 kHz
Number of Turns	Np = 2, Ns = 4, split sec.	same
Core Loss, P_c	44.5 W @ 25°C	35 W @ 25°C 30 W @ 110°C 28 W @ 160°C 27 W @ 200°C
Copper Loss, P_{cu} (Meas. at xfmr terminals)	4.14 W @ 10 A rms, 220°C 9.31 W @ 15 A rms, 220°C	9 W @ 10 A rms, 220°C 23 W @ 15 A rms, 220°C
Efficiency	98.06 % @ 2.5 kVA	98.49 % @ 2.45 kVA 98.47 % @ 3.43 kVA
kVA Rating	2.5 kVA	3.43 kVA measured Output Power : 3.22 kW
Temperature Rise in °C (Max. noted on Core or Copper)	52.8°C (For Core)	35°C @ 2.45 kVA (1 hr) 47°C @ 3.43 kVA (1 hr)
Number of Core	30	same
Weight	3.17 lbs	4.19 lbs
Length	10.75 in	same
Width	3.13 in	same
L_{leak} (prim. referred) (Meas. at xfmr terminals)	376 nH	403 nH (660 nH)
L_{mag}	14.72 mH	12.0 mH
Relative Permeability, μ_r	30,000	-------

3.6 Suitability for Space Applications

Co-axial winding transformers proved to be a good choice for high power density and high frequency applications. They have a more predictable performance compared with conventional transformers. In addition, the leakage inductance of the transformer can be controlled easily to suit a specific application.

For space applications, one major concern is the extraction of heat from power apparatus to prevent excessive heating and hence damaging of these units. Because of the vacuum environment, the only way to extract heat is by using a cold plate.

One advantage of co-axial winding transformers is that the surface area available to extract heat from is very large compared to conventional transformers. This stems from the unique structure of the co-axial transformer where the whole core surface area is exposed and can be utilized for cooling effectively. This is a crucial issue here since most of the losses, as shown earlier, are core losses.

The transformer designed in this project has a total loss of about 35 W at rated kVA. The total surface area of the transformer can be calculated from the transformer geometry as,

$$A_s = \pi OD_{core} l_{core} = 760\ cm^2 \tag{3.9}$$

Hence, the total loss per unit surface area is,

$$P_{l\_s} = \frac{P_{total}}{A_s} = \frac{35}{760} = 0.047\ W/cm^2 \tag{3.10}$$

which is quite small and can be extracted easily. On the other hand, the total loss per unit length is,

$$P_{l\_l} = \frac{P_{total}}{l_{core}} = \frac{35}{38.1} = 0.92\ W/cm \tag{3.11}$$

which is almost 1 W/cm. Again, this amount of power can be extracted easily by a cold plate cooling mechanism.

One possible structure for cold plate cooling in space applications is shown in Fig. 3.13. In this figure, the cold plate is mounted along the transformer sides and a copper foil is

wrapped over the cores and clamped in the middle. Note here that since the core material has very high permeability, there will be nearly no flux penetrating the copper foil, and hence, no additional losses. This arrangement has the advantage of small additional weight to the transformer weight.

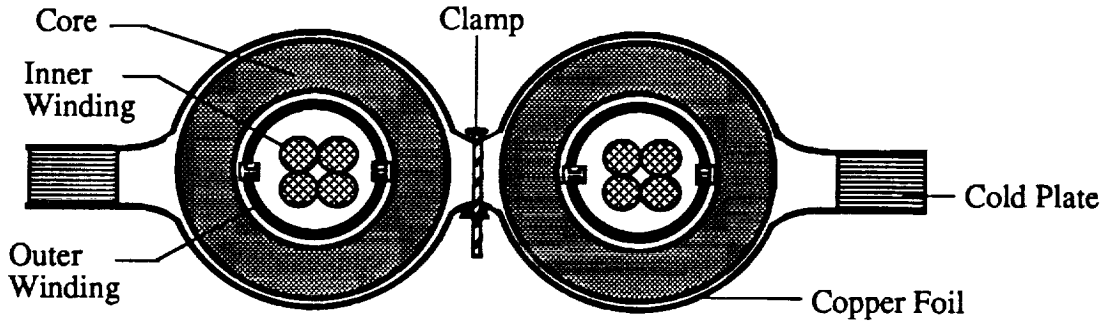

Fig. 3.13 One possible cold plate cooling for space applications

Another possible cold plate cooling scheme is shown in Fig. 3.14. An aluminum base plate is placed between the two cores and copper foils are used on each side to clamp the transformer to the plate. The aluminum plate has two flat portions, on top and on bottom, which can be used for mounting the transformer on a cold plate.

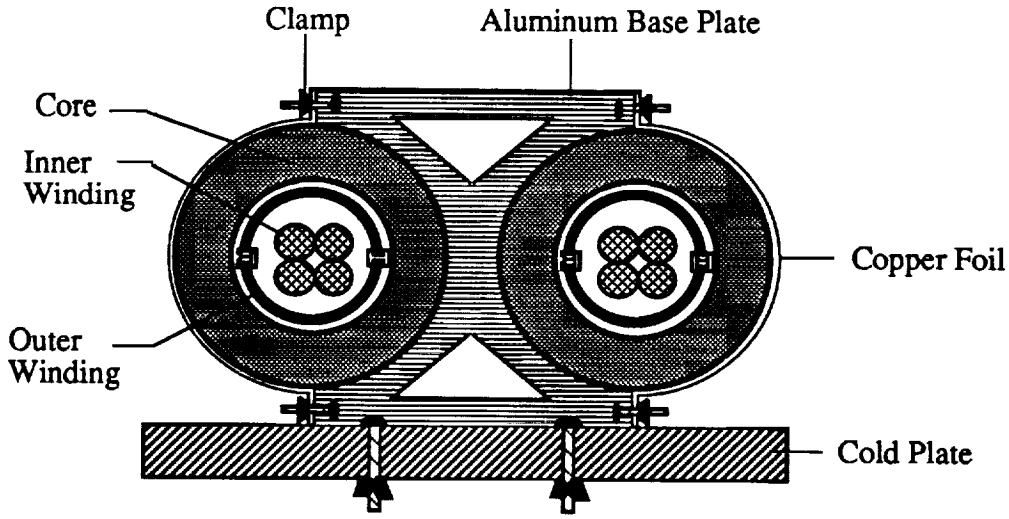

Fig. 3.14 Another possible cold plate cooling for space applications

REFERENCES

[1] M. H. Kherulawala, D. W. Novotny, D. M. Divan, "Design Considerations for High Frequency Transformers," IEEE-PESC Rec., pp. 734-742, 1990.

[2] M. H. Kherulawala, R. W. Gascoigne, D. M. Divan, E. Bauman, "Performance Characterization of a High Power Dual Active Bridge DC/DC Converter," IEEE-IAS Rec., pp. 1267-1283, 1990.

[3] H. L. N. Weigman, D. M. Divan, D. W. Novotny, R. Mohan, " A ZVS Dual Resonant Converter for Battery Charging Applications," IEEE-PESC Rec., 1991.

[4] M. Rauls, "Analysis and design of High Frequency Co-Axial Winding Power Transformers," M. S. Thesis, University of Wisconsin-Madison, 1992.

[5] T. A. Lipo, "Electromagnetic Design of AC Machines," Class Notes, University of Wisconsin-Madison, 1992.

[6] G. R. Slemon, Magneto electric Devices, Second Edition, John Wiley and Sons, 1990.

[7] MAGNETICS' Tape Wound Cores Catalogue, 1990.

[8] ARNOLD's Tape Wound Cores Catalogue.

[9] ALLIED SIGNAL's METGLAS Alloys Catalogue.

[10] COTRONICS Corp. Adhesive Ceramics and High Temperature Materials Handbook, 1992.

[11] OMEGA Inc. Temperature Handbook.

[12] J. F. Fritz, J. J. Clark, "Effects of Temperature on Magnetic Properties of Nickel-Iron Alloys: over temperature range of -60 to 250°C," Electrical Manufacturing, Vol. 62, November 1958, pp. 135-139.

[13] P. D. Agarwal, "Eddy Current Losses in Solid and Laminated Iron," AIEE Trans., Vol. 78, Part 1, pp. 169-181, 1960.

APPENDIX A

Magnetic Core Loss Data

In this appendix, the loss curves for the magnetic materials used in chapter 2 are included. These loss curves were obtained from the MAGNETICS and the ALLIED SIGNAL catalogues.

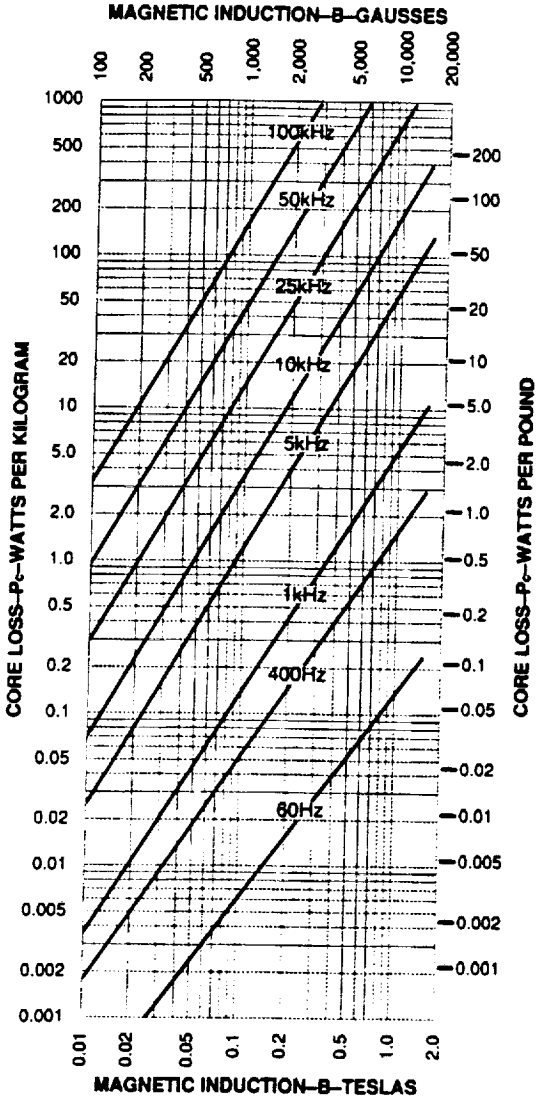

(a)

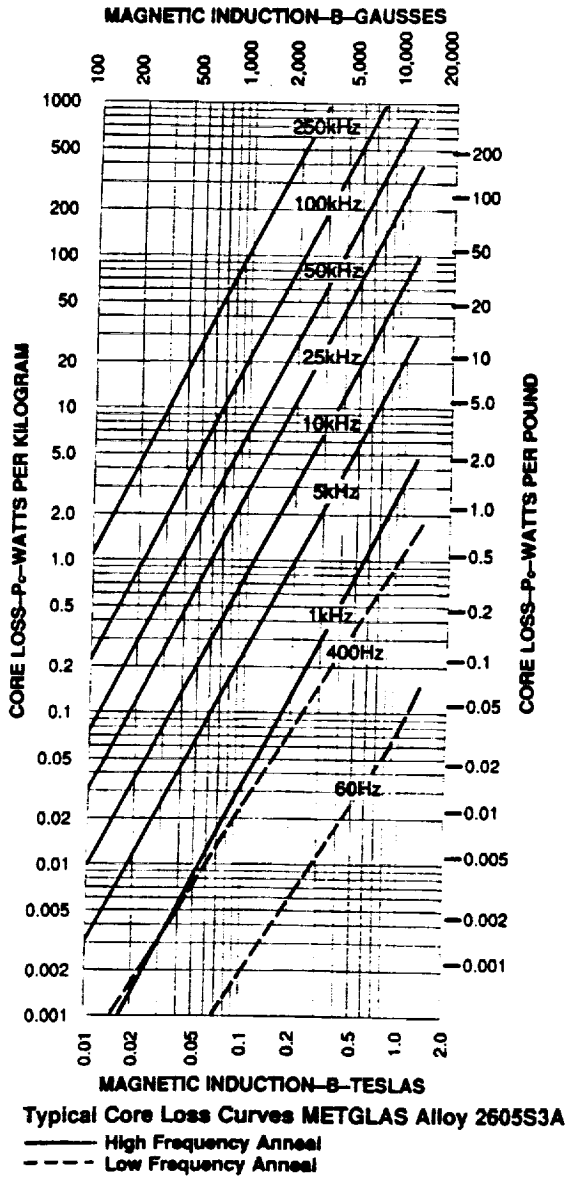

(b)

Fig. A.1 Core loss data for the METGLAS 1 mil alloys (a) 2605 SC (b) 2605 S3A

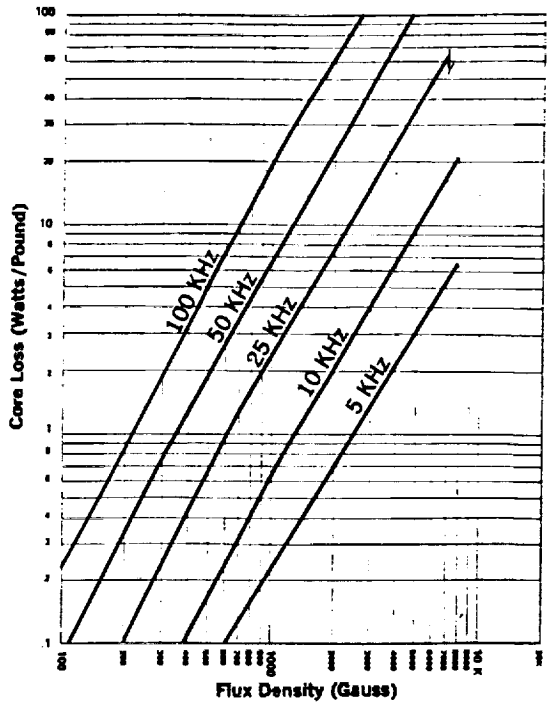

Fig. A.2 Core loss data for Square Permalloy 1 mil tape

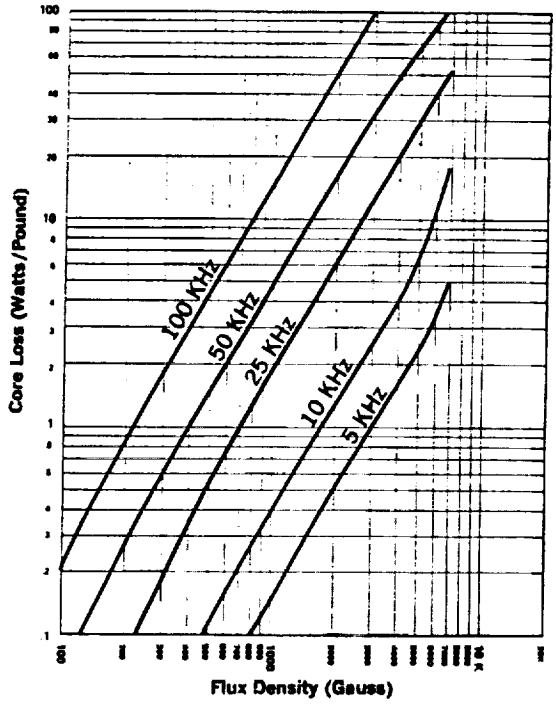

Fig. A.3 Core loss data for Supermalloy 1 mil tape

APPENDIX B

Selecting Secondary Wire Size

As noted in chapter 2 (§2.4), the secondary wire size selected was an AWG 12 wire. This is based on the fact that given the current density specifications for the secondary winding and the total secondary current, the total copper cross sectional area need to be > 0.025 cm^2 (4934 cir mils). An AWG 13 wire may seem to be a reasonable wire size, but in fact it is not. This is due to the fact that the skin effect at high frequencies forces the current to flow within one skin depth of the copper wire. Hence, the actual utilized copper area is a one skin depth thick shell, as shown in Fig. B.1.

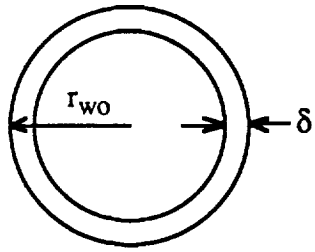

Fig. B.1: Utilized copper cross sectional area

The effective cross sectional area for the copper shell in Fig. B.1 is given by,

$$A_{wire} = \pi \left[r_{wo}^2 - (r_{wo} - \delta)^2 \right] = \pi \delta \, (2 \, r_{wo} - \delta) \qquad \text{(B.1)}$$

Solving for r_{wo},

$$r_{wo} = \frac{A_{wire}}{2 \pi \delta} + \frac{\delta}{2} \qquad \text{(B.2)}$$

Using the data in §2.4, the wire cross sectional area is 0.025 cm^2 while the skin depth at 20 kHz is 0.051 cm. Hence, the wire outer diameter is 0.207 cm (0.0815 inches). A wire size with a similar dimension is the AWG 12 wire where the outer diameter is 0.0808 inches. For a stranded AWG 12 wire, the actual radius is in the order of 0.1 inches. With a 10 mil insulation, the total wire diameter is 0.12 inches (0.3 cm).

APPENDIX C

Excel Spread Sheet Listings

In this appendix, the Excel spread sheet data listings used for transformer design evaluation in chapter 2 are included.

Possible Cores : (Magnetics' & Arnold's Catalogs)

Required Core X-section = 17.595 cm^2

Np = 2 ; Ns = 4

B = 0.4 T (Bsat. @ 300 C = 0.55 T)

f = 20 KHz

Core Lamination = 1 mil, Cores are unboxed

Core #	ID (in)	OD (in)	HT (in)	Ac (1 mil) cm^2	Lm (cm)	Nc	Lc (in)	Volume cm^3
53057	0.625	0.750	0.125	0.038	5.48	464	58.00	98.623
53063	0.625	0.875	0.125	0.076	5.48	232	29.00	98.623
53002	0.650	0.900	0.125	0.076	6.18	232	29.00	108.906
53033	0.625	0.875	0.25	0.151	5.98	116	29.00	104.746
53076	0.625	1.000	0.188	0.171	6.48	102	19.18	113.024
53296	0.600	0.900	0.25	0.192	5.98	96	24.00	104.483
53007	0.625	1.000	0.25	0.227	6.48	78	19.50	114.735
53167	0.625	1.125	0.25	0.303	6.98	58	14.50	122.667
53094	0.625	1.000	0.375	0.34	6.48	52	19.50	114.566
53133	0.650	1.150	0.375	0.454	7.18	38	14.25	123.869
53061	0.75	1.000	0.25	0.151	6.98	116	29.00	122.262
53106	0.75	1.125	0.188	0.171	7.48	102	19.18	130.466
53084	0.75	1.125	0.25	0.227	7.48	78	19.50	132.441
53318	0.75	1.250	0.25	0.303	7.98	58	14.50	140.241
53034	0.75	1.125	0.375	0.34	7.48	52	19.50	132.246
53186	0.75	1.250	0.375	0.454	7.98	38	14.25	137.671
53481	0.75	1.250	0.5	0.605	7.98	30	15.00	144.837
53514	0.75	1.500	0.375	0.681	8.97	26	9.75	158.823
T 5762	0.75	1.25	1.00	1.209	7.98	14	14.00	135.069

Core Loss for Each Suggested Material :

			MG 2605 S3A (1 mil)			SQ Permalloy (1 mil)			Supermalloy (1 mil)		
Core #	Lc (in)	Volume cm^3	k	Wt (lbs)	Losses (W)	k	Wt (lbs)	Losses (W)	k	Wt (lbs)	Losses (W)
53057	58.00	96.623	0.0161	1.56	21.78	0.0192	1.86	33.39	0.0192	1.86	29.68
53063	29.00	96.623	0.0161	1.56	21.78	0.0192	1.86	33.39	0.0192	1.86	29.68
53002	29.00	108.966	0.0161	1.75	24.56	0.0192	2.09	37.66	0.0192	2.09	33.47
53033	29.00	104.746	0.0161	1.69	23.61	0.0192	2.01	36.20	0.0192	2.01	32.18
53076	19.18	113.024	0.0161	1.82	25.48	0.0192	2.17	39.06	0.0192	2.17	34.72
53296	24.00	104.483	0.0161	1.68	23.55	0.0192	2.01	36.11	0.0192	2.01	32.10
53007	19.50	114.735	0.0161	1.85	25.86	0.0192	2.20	39.65	0.0192	2.20	35.25
53167	14.50	122.667	0.0161	1.97	27.65	0.0192	2.36	42.39	0.0192	2.36	37.68
53094	19.50	114.566	0.0161	1.84	25.82	0.0192	2.20	39.59	0.0192	2.20	35.19
53133	14.25	123.869	0.0161	1.99	27.92	0.0192	2.38	42.81	0.0192	2.38	38.05
53061	29.00	122.262	0.0161	1.97	27.56	0.0192	2.35	42.25	0.0192	2.35	37.56
53106	19.18	130.466	0.0161	2.10	29.41	0.0192	2.50	45.09	0.0192	2.50	40.08
53084	19.50	132.441	0.0161	2.13	29.85	0.0192	2.54	45.77	0.0192	2.54	40.69
53318	14.50	140.241	0.0161	2.26	31.61	0.0192	2.69	48.47	0.0192	2.69	43.08
53034	19.50	132.246	0.0161	2.13	29.81	0.0192	2.54	45.70	0.0192	2.54	40.63
53188	14.25	137.671	0.0161	2.22	31.03	0.0192	2.64	47.58	0.0192	2.64	42.29
53481	15.00	144.837	0.0161	2.33	32.65	0.0192	2.78	50.06	0.0192	2.78	44.49
53514	9.75	158.823	0.0161	2.56	35.80	0.0192	3.05	54.89	0.0192	3.05	48.79
T 5762	14.00	135.069	0.0161	2.17	30.44	0.0192	2.59	46.68	0.0192	2.59	41.49

Transformer Data for Each Core

Note: Temp. effect on copper resistance --> 70.2 % increase in resistance

Wire Insulation : (> 300 C)

(AWG=12) (Is=10 A) 0.0738 (lbs/m)

Core #	OD (in)	Lc (m)	L_turn (m)	L_lk (nH) (primary)	L_wire (m)	R_wire (Ohm)	Wire_Loss (W)	Wire_wgt (lbs)	R_tube (Ohm)	Tube_Loss (W)	Tube_wgt (lbs)
53057	0.750	1.473	1.593	1031.71	6.372	9.41E-02	9.41	0.863	0.00484845	1.939	0.216
53063	0.875	0.737	0.876	567.54	3.505	5.18E-02	5.18	0.475	0.00266711	1.067	0.119
53002	0.900	0.737	0.880	570.12	3.521	5.20E-02	5.20	0.477	0.00267925	1.072	0.119
53033	0.875	0.737	0.876	567.54	3.505	5.18E-02	5.18	0.475	0.00266711	1.067	0.119
53076	1.000	0.487	0.647	418.84	2.587	3.82E-02	3.82	0.350	0.00196831	0.787	0.088
53296	0.900	0.610	0.753	487.86	3.013	4.45E-02	4.45	0.408	0.00229269	0.917	0.102
53007	1.000	0.495	0.655	424.17	2.620	3.87E-02	3.87	0.355	0.00199336	0.797	0.089
53167	1.125	0.368	0.548	354.83	2.191	3.24E-02	3.24	0.297	0.00166752	0.667	0.074
53094	1.000	0.495	0.655	424.17	2.620	3.87E-02	3.87	0.355	0.00199336	0.797	0.089
53133	1.150	0.362	0.545	353.30	2.182	3.22E-02	3.22	0.296	0.00166034	0.664	0.074
53061	1.000	0.737	0.896	580.46	3.585	5.30E-02	5.30	0.486	0.00272783	1.091	0.121
53106	1.125	0.487	0.667	431.76	2.666	3.94E-02	3.94	0.361	0.00202903	0.812	0.090
53084	1.125	0.495	0.675	437.09	2.699	3.99E-02	3.99	0.366	0.00205408	0.822	0.091
53318	1.250	0.368	0.568	367.75	2.271	3.36E-02	3.36	0.308	0.00172824	0.691	0.077
53034	1.125	0.495	0.675	437.09	2.699	3.99E-02	3.99	0.366	0.00205408	0.822	0.091
53188	1.250	0.362	0.561	363.64	2.246	3.32E-02	3.32	0.304	0.00170891	0.684	0.076
53481	1.250	0.381	0.580	375.98	2.322	3.43E-02	3.43	0.315	0.0017669	0.707	0.079
53514	1.500	0.248	0.487	315.45	1.948	2.88E-02	2.88	0.264	0.00148245	0.593	0.066
T 5762	1.25	0.356	0.555	359.53	2.220	3.28E-02	3.28	0.301	0.00168959	0.676	0.075

Final Designed Transformer

	MG 2605 S3A (1 mil)			SQ Permalloy (1 mil)			Supermalloy (1 mil)		
Core #	Total Wgt (lbs)	Total Loss (W)	Efficiency (%)	Total Wgt (lbs)	Total Loss (W)	Efficiency (%)	Total Wgt (lbs)	Total Loss (W)	Efficiency (%)
53057	2.635	33.13	98.67	2.93	44.75	98.21	2.93	41.04	98.36
53063	2.149	28.02	98.88	2.45	39.64	98.41	2.45	35.93	98.56
53002	2.351	30.83	98.77	2.69	43.93	98.24	2.69	39.75	98.41
53033	2.280	29.85	98.81	2.60	42.45	98.30	2.60	38.42	98.46
53076	2.258	30.08	98.80	2.61	43.67	98.25	2.61	39.33	98.43
53296	2.192	28.92	98.84	2.52	41.48	98.34	2.52	37.47	98.50
53007	2.291	30.53	98.78	2.65	44.32	98.23	2.65	39.91	98.40
53167	2.346	31.55	98.74	2.73	46.30	98.15	2.73	41.59	98.34
53094	2.288	30.49	98.78	2.64	44.26	98.23	2.64	39.86	98.41
53133	2.364	31.81	98.73	2.75	46.70	98.13	2.75	41.94	98.32
53061	2.575	33.95	98.64	2.95	48.64	98.05	2.95	43.95	98.24
53106	2.552	34.16	98.63	2.96	49.84	98.01	2.96	44.83	98.21
53084	2.589	34.66	98.61	3.00	50.58	97.98	3.00	45.50	98.18
53318	2.642	35.66	98.57	3.08	52.51	97.90	3.08	47.13	98.11
53034	2.586	34.62	98.62	3.00	50.51	97.98	3.00	45.44	98.18
53188	2.597	35.03	98.60	3.02	51.58	97.94	3.02	46.29	98.15
53481	2.725	36.78	98.53	3.17	54.19	97.83	3.17	48.63	98.05
53514	2.887	39.27	98.43	3.38	58.36	97.67	3.38	52.26	97.91
T 5762	2.551	34.40	98.62	2.97	50.64	97.97	2.97	45.45	98.18

APPENDIX D

Temperature Effect on Magnetic Properties of Supermalloy

The temperature effect data given in this appendix was taken from reference [12].

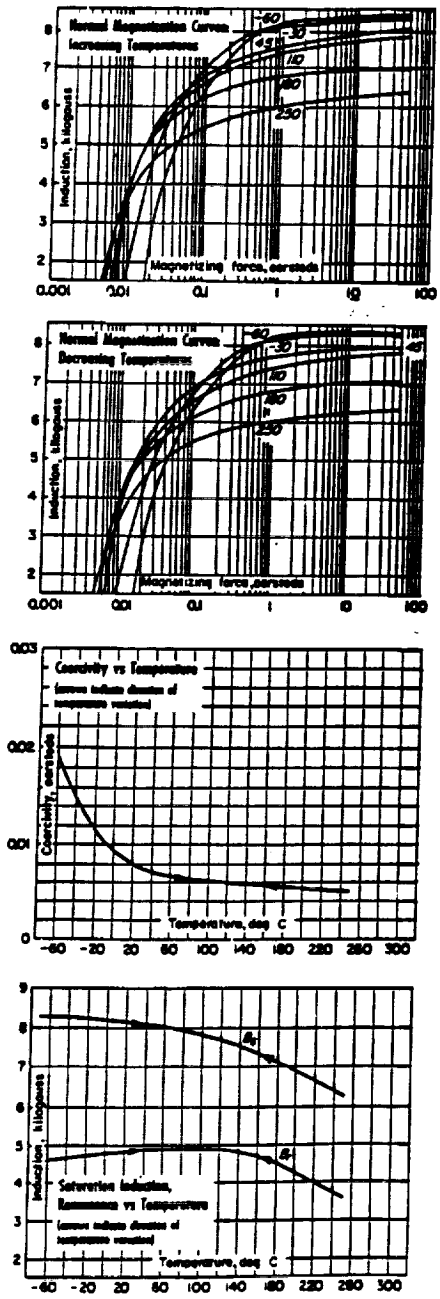

Fig. D.1 Temperature effect on the magnetic properties of Supermalloy